Kaunas University of Technology

Faculty of Mechanical Engineering and Design

Development of Robotic System Integrating Hand-Held 3D Scanner for Capturing Geometry of Human Limbs and Optimizing Scanning Parameters

Master's Final Degree Project

Donatas Akulovas

Project author

Assist. Prof. Dr. Arūnas Kleiva

Supervisor

Kaunas, 2025

Kaunas University of Technology

Faculty of Mechanical Engineering and Design

Development of Robotic System Integrating Hand-Held 3D Scanner for Capturing Geometry of Human Limbs and Optimizing Scanning Parameters

Master's Final Degree Project

Mechatronics (6211EX017)

Donatas Akulovas

Project author

Assist. Prof. Dr. Arūnas Kleiva

Supervisor

Assist. Prof. Dr. Darius Mažeika

Reviewer

Kaunas, 2025

Kaunas University of Technology

Faculty of Mechanical Engineering and Design

Donatas Akulovas

Development of Robotic System Integrating Hand-Held 3D Scanner for Capturing Geometry of Human Limbs and Optimizing Scanning Parameters

Declaration of Academic Integrity

I confirm the following:

1. I have prepared the final degree project independently and honestly without any violations of the copyrights or other rights of others, following the provisions of the Law on Copyrights and Related Rights of the Republic of Lithuania, the Regulations on the Management and Transfer of Intellectual Property of Kaunas University of Technology (hereinafter – University) and the ethical requirements stipulated by the Code of Academic Ethics of the University;

2. All the data and research results provided in the final degree project are correct and obtained legally; none of the parts of this project are plagiarised from any printed or electronic sources; all the quotations and references provided in the text of the final degree project are indicated in the list of references;

3. I have not paid anyone any monetary funds for the final degree project or the parts thereof unless required by the law;

4. I understand that in the case of any discovery of the fact of dishonesty or violation of any rights of others, the academic penalties will be imposed on me under the procedure applied at the University; I will be expelled from the University and my final degree project can be submitted to the Office of the Ombudsperson for Academic Ethics and Procedures in the examination of a possible violation of academic ethics.

Donatas Akulovas

Confirmed electronically

Kaunas University of Technology

Faculty of Mechanical Engineering and Design

Task of the Master's Final Degree Project

Given to the student – Donatas Akulovas

1. Title of the Project

Development of Robotic System Integrating Hand-Held 3D Scanner for Capturing Geometry of Human Limbs and Optimizing Scanning Parameters

(In English)

Robotinės sistemos, integruojančios rankinį 3D skaitytuvą, skirtą žmogaus galūnių geometrijai fiksuoti ir nuskaitymo parametrams optimizuoti, kūrimas

(In Lithuanian)

2. Aim and Tasks of the Project

Aim: to develop a system combining a hand-held 3D scanner with a robotic arm to capture the geometry of human limbs.

Tasks:

1. to fabricate an adapter to mount the Creaform HandyScan 700 onto the ABB IRB 1200 robot arm;
2. to configure the ABB IRB 1200 for safe and precise movements around a human subject;
3. to adapt the system for incremental editing and further development of an automated 3D scanning system in clinical or industrial settings;
4. to conduct post-processing work on scanned models and compare results;
5. to discuss the potential economic and environmental benefits of an automated 3D scanning system in clinical or industrial settings.

3. Main Requirements and Conditions

Utilizes ABB RobotStudio software to control the robot arm, SolidWorks, Fusion 3D and Meshmixer software for design and mesh editing. The robot arm ABB IRB 1200 and 3D scanner Creaform HandyScan 700 will be used. The adapter for holding the scanner will be 3D printed using PLA. VXelements 12 software will be used to conduct the scans and analyse results.

4. Additional Requirements for the Project, Report and its Annexes

Not Applicable.

Project author	Donatas Akulovas		07-03-2025
	(Name, Surname)	*(Signature)*	*(Date)*
Supervisor	Arūnas Kleiva		07-03-2025
	(Name, Surname)	*(Signature)*	*(Date)*
Head of study field programs	Regita Bendikienė		07-03-2025
	(Name, Surname)	*(Signature)*	*(Date)*

Akulovas Donatas. Development of Robotic System Integrating Hand-Held 3D Scanner for Capturing Geometry of Human Limbs and Optimizing Scanning Parameters. Master's Final Degree Project, supervisor assist. prof. dr. Arūnas Kleiva; Faculty of Mechanical Engineering and Design, Kaunas University of Technology.

Study field and area (study field group): Production and Manufacturing Engineering (E10), Engineering Sciences (E).

Keywords: laser triangulation; hand-held 3D scanner; scanning automation; human limb anthropometry; 3D model accuracy.

Kaunas, 2025. 56 p.

Summary

The goal of this study was to implement the 3D scanner HandyScan 700 on the robot arm IRB 1200 for human limb scanning and evaluate the effect scanning and automation parameters have on recorded meshes. Scanning of a 3D printed replica arm was evaluated using industry standard metrics of surface area covered by the point cloud and its standard deviation, which shows how far away on average are the captured points from the reference. To ensure consistent test results, a static hand replica was used instead of a real one, which had to be scanned in a top and bottom pass and then merged due to insufficient robot reach. Four main experiments were conducted; one assessed the effects of laser exposure time for two different surface finishes (white-glossy, grey-matte), where it was found that higher times are better suited for a glossy surface, lower times – matte surface. Another experiment tested scan repeatability by comparing 7 scans under the same conditions to each other and to a reference mesh, finding that scanner noise was very low at 0.0277 mm for the matte finish. Grey-matte surface finish had 50% lower noise and on average more stable standard deviation than the white-glossy one, demonstrating the negative effects of a reflective surface. Robot speed was also evaluated, with highest accuracy scans being reached while using 100 mm/s speed (preset v100) and 0.2 mm resolution, where standard deviation was as low as 0.039 mm. A recommended compromise between speed and quality is a resolution of 0.6-1 mm and speeds of 500-800 mm/s, which resulted in 0.05-0.1 mm standard deviation and average scan time of 23 seconds (one side). Another test was aimed to quantify how the auto setup compared to human operators, where it was found that there is no difference in accuracy of results, but the auto setup is ~3 times faster. The automated setup was able to match results of similar studies that were using manual scanning methods, as well as of those that aimed to automate scanning. Major limiting factors for scanning of real hands were motion blur and angle change between top and bottom scans, further research is needed regarding limb support during scanning, as well as different robot arm use to support 360° movement around the subject. Rough cost calculations showed that implementing this auto 3D scanning system would cost €65,000 and if used instead of plaster casting for lost limb measurement would result in cost savings of €87 per patient, which would also prevent >1 kg of plaster waste per measurement.

Akulovas Donatas. Robotinės sistemos, integruojančios rankinį 3D skaitytuvą, skirtą žmogaus galūnių geometrijai fiksuoti ir nuskaitymo parametrams optimizuoti, kūrimas. Magistro baigiamasis projektas, vadovas asist. dr. Arūnas Kleiva; Kauno technologijos universitetas, Mechanikos inžinerijos ir dizaino fakultetas.

Studijų kryptis ir sritis (studijų krypčių grupė): Gamybos inžinerija (E10), Inžinerijos mokslai (E).

Reikšminiai žodžiai: lazerinė trianguliacija; rankinis 3D skeneris; skenavimo automatizavimas; žmogaus galūnių antropometrija; 3D modelio tikslumas.

Kaunas, 2025. 56 p.

Santrauka

Šio tyrimo tikslas buvo įdiegti 3D skenerį HandyScan 700 ant roboto rankos IRB 1200 žmogaus galūnių skenavimui ir įvertinti skenavimo bei automatizavimo parametrų poveikį nuskaitomiems rezultatams. 3D spausdintos kopijos skenavimas buvo įvertintas naudojant pramonės standartines metrikas: paviršiaus plotą, kurį dengia taškinis debesis ir jo standartinį nuokrypį, kuris parodo, vidutiniškai kaip toli užfiksuoti taškai yra nuo atskaitinio paviršiaus. Siekiant užtikrinti nuoseklius bandymų rezultatus, vietoj tikros buvo naudojama statinė rankos kopija, kurią dėl nepakankamo roboto pasiekiamumo reikėjo nuskenuoti iš dviejų pusių – viršaus bei apačios, o tada sujungti. Buvo atlikti keturi pagrindiniai eksperimentai; vienas jų vertino lazerio ekspozicijos laiko poveikį dviem skirtingoms paviršiaus apdailoms (baltai blizgiai, pilkai matinei), kur nustatyta, jog didesnis laikas geriau tinka blizgiam paviršiui, žemesnis laikas – matiniam. Kitame eksperimente buvo išbandytas skenavimo pakartojamumas, lyginant 7 nuskaitymus tomis pačiomis sąlygomis vieną su kitu ir su atskaitiniu paviršiumi, kur nustatyta, kad skaitytuvo triukšmas buvo itin mažas – 0,0277 mm matinei apdailai. Pilka matinio paviršiaus apdaila turėjo 50 % mažesnį triukšmą bei stabilesnį standartinį nuokrypį nei balta blizgi, o tai rodo neigiamą atspindinčio paviršiaus poveikį. Taip pat buvo įvertintas roboto greitis, kai didžiausias tikslumas pasiektas naudojant 100 mm/s greitį (iš anksto nustatytas v100 nustatymas) ir 0,2 mm rezoliuciją, kur standartinis nuokrypis siekė net 0,039 mm. Rekomenduojamas kompromisas tarp greičio ir kokybės yra 0,6-1 mm skiriamoji geba ir 500-800 mm/s greitis, tada standartinis nuokrypis liko tarp 0,05–0,1 mm, o vidutinis nuskaitymo laikas – 23 sekundės (tik viena pusė). Kitas bandymas buvo skirtas kiekybiškai įvertinti, kaip automatinė sistema prilygsta žmonėms operatoriams, kur buvo nustatyta, kad rezultatų tikslumas nesiskiria, tačiau automatinė sąranka yra ~3 kartus greitesnė. Automatizuota sistema atitiko kokybės rezultatus panašių tyrimų, kuriuose buvo naudojami rankinio skenavimas, taip pat tuos, kuriuose skenavimas automatizuotas. Pagrindiniai veiksniai, ribojantys realių rankų nuskaitymą buvo judesio sulieti taškai ir kampo pokytis tarp viršutinio ir apatinio skenavimų, reikia tolesnių tyrimų, susijusių su galūnių įtvirtinimu skenavimo metu, taip pat skirtingos roboto rankos, kuri palaiko 360° judėjimą aplink objektą, testavimas. Apytiksliai apskaičiavus išlaidas paaiškėjo, kad šios automatinės 3D skenavimo sistemos įdiegimas kainuotų 65 000 eurų, o jei ji būtų naudojama vietoj gipso liejimo prarastų galūnių matavimui, vienam pacientui būtų sutaupyti 87 eurai, o tai taip pat padėtų išvengti daugiau nei 1 kg gipso atliekų kiekvieną matavimą.

Table of Contents

List of Figures

List of Tables

Introduction

Accurately reading the complex shape of a limb is the first and most important step in designing a prosthetic, orthotic or orthopaedic wearable device, yet many clinics rely manual measurement, plaster casting and other archaic methods, which have long since been abandoned in other industries. For example, plaster casting uses impregnated bandages that are slow to apply, messy and produce significant waste. They also rarely return a perfect result, the cast can shift as it dries and even a 2 mm drift in the socket can cause pressure spots which are uncomfortable for the user, since the process is long and tedious, the measurements are not easy to repeat. Handheld 3D scanners can provide better, easily below 1 mm error, cleaner and faster results, but require larger upfront investment and some level of operator skill. For 3D scanning, the main time limiter is user skill, since knowing how to move the scanner, what distance to keep it at, how to rotate it, how fast I can be moved are all knowledge that can increase speed tremendously. Compared to manual methods, digitised methods can manufacture a prototype within an hour, so the high compatibility of 3D scanning with 3D printing is a huge strength. While medium-level scanners can be used plug and play, where all settings are kept to factory ones, their results will hardly be optimal. Despite the abundance of relevant scanning parameters, none of the analysed studies explored this topic in detail, such as what are the ideal scanning parameters for limb scanning. In addition, handheld scanner movement automation was not explored in studies, with most automated systems using photogrammetry instead. There is merit in automating handheld scanner movement however, as such scanners have an ideal distance to object window, maximum view angle change and others, none of which a human operator can follow consistently without significant experience. Theoretically, a scenario where a robot controls all movement, following the same path near identically every time should be the optimal way to test different scanner parameters in search of the best configuration. That is why, in this work the HandyScan 700 handheld scanner is to be combined with the robot arm IRB 1200 to push forward the general understanding of each parameter's influence on retrieved meshes. By providing both detailed scanning parameters and an easily repeatable automated workflow, this study will be an example to other works where handheld scanner settings are relevant.

Aim: to develop a system combining a hand-held 3D scanner with a robotic arm to capture the geometry of human limbs.

Tasks:

1. to fabricate an adapter to mount the Creaform HandyScan 700 onto the ABB IRB 1200 robot arm;
2. to configure the ABB IRB 1200 for safe and precise movements around a human subject;
3. to adapt the system for incremental editing and further development of an automated 3D scanning system in clinical or industrial settings;
4. to conduct post-processing work on scanned models and compare results;
5. to discuss the potential economic and environmental benefits of an automated 3D scanning system in clinical or industrial settings.

Hypothesis: can automating human limb scanning with a robot arm improve measurement accuracy?

1. Analysis of 3D Scanning of the Human Body

1.1. 3D Scanning Use on Humans

The use of 3D scanning is something that is applied in many different fields nowadays. The military sector was one of the first and biggest users of this technology in the form of laser imaging, detection and ranging (LIDAR). LIDAR has been used extensively for long-range 3D mapping of the environment. 3D scanning is also used in architecture to retrieve outdoor or indoor 3D models of buildings which is quite useful for planning renovation or remodelling or just taking measurements. Another exciting use is found in manufacturing, design of custom parts, especially for cases where measuring is complicated, is made much easier by scanning the object and then inspecting the model. It is also used a lot in large scale manufacturing, for example, to scan a production line to find defective parts. While there are other mainstream uses for 3D scanning, these are the main ones.

Although scanning is quite an old and widely known technology, it has many new and promising applications. The fashion and apparel industry has been exploring the use of 3D scanning in recent years. They use full-body scans to retrieve precise measurements of a person to design custom clothing. A digital avatar of someone can also be used more creatively in things like virtual dressing rooms [1, 31]. Another interesting use is for the preservation of art and cultural heritage [2]. Archaeologists use scanners to record historical monuments, which makes that information easier to share between experts. Artists sometimes use scans to digitise their 3D artworks like sculptures or installations. It is even being used in forensic science, where in some cases detectives can use 3D scanners to capture the entire crime scene quickly [32]. This allows to preserve the surroundings as they were and more people to analyse the scene, in greater detail. Research shows that this can improve origin estimation for bloodstains [3]. Finally, an implementation particularly exciting is the use of 3D scanning to create models for virtual reality [4]. A recent review work highlighted potential uses of 3D scanning in various industries; the figure below (Fig. 1) illustrates their findings [2].

Fig. 1. Fields That Apply 3D Scanning and the Way it is Used [2]

One huge sphere not yet discussed is the healthcare sector, which is arguably the most relevant to the future of 3D scanning. As it stands, the main use of scanning in the healthcare industry is in dentistry, where a visit to the clinic typically starts with an intraoral scan of the patient‘s mouth. These scans retrieve a precise mapping of the teeth and gums, allowing dentists to rehearse any procedure in advance [5]. Aside from dentistry, 3D scanning is also being used to design custom prosthetics to maximise patient comfort. However, the use of scanning in healthcare is still very limited relative to how large the sector is, despite the many emerging applications that are being actively researched. While perfect fit prosthetics are seeing some use, custom braces, casts and orthopaedic aids are significantly less popular. Some studies argue that this is a direction worth exploring and have even shown positive results from the use of custom hip braces, for example (see Fig. 2) [6]. In dermatology, scans can also be used to monitor patients‘ skin condition over long periods, which ensures that human error is less prevalent in some cases [7]. This helps to more accurately track the progression of a healing wound or disease. Posture can also be tracked this way, giving more precise data than pictures, which should help in the recovery process. A new interesting use of this technology is to scan a patient before some surgery, as part of the preparation. Doctors can analyse the 3D model of the surgery area and do simulations, which makes them better prepared [8]. This use case in particular should gain more traction as software for such things is developed. Due to these factors, it can be said that the use of 3D scanning in medicine has great potential yet untapped.

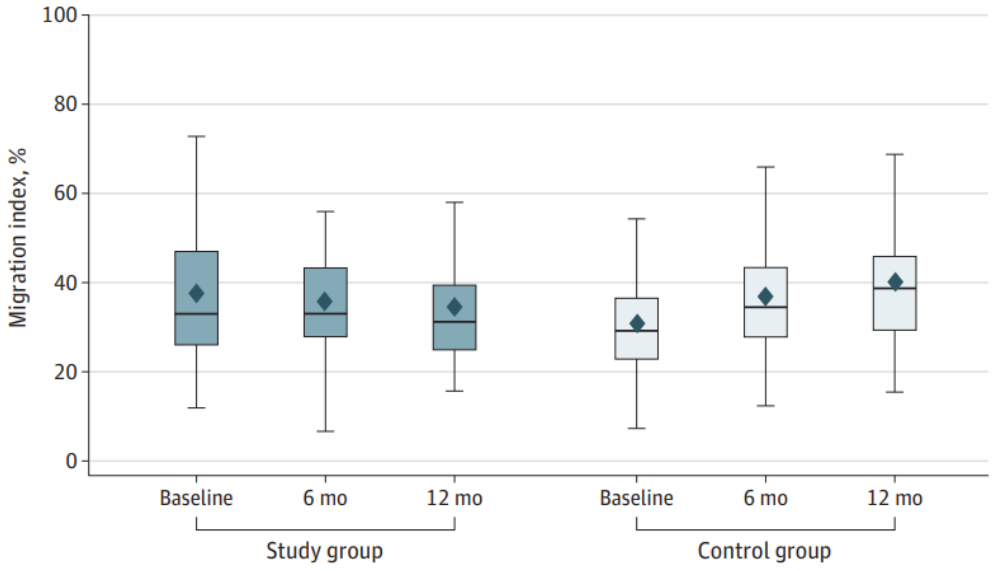

Fig. 2. Hip Migration Index of Patients with Custom Hip Braces Over 12 Months (lower is better) [6]

Among the different applications of 3D scanning, people are possibly the hardest to scan. The human body has many complex surfaces and details. This kind of geometry, combined with the nature of a living being never staying perfectly still, proves to be quite challenging [9]. Movement caused by heartbeat, breathing and nerve-related factors, can cause scans to lose out on accuracy and capture artefacts. Currently, there are three main methods to solve this, one is to use photogrammetry as the 3D scanning method, which can do a full scan almost instantaneously if using a multi-camera setup. The problem with this method is that it can be very costly due to the requirement of at least 30 cameras to capture many angles at once for reliable results [9, 11]. Another way would be to simply have the person lie down, but in order to get the full model, we would have to stitch two scans together [6, 11]. This is overly time consuming and loses scan accuracy which could be less of a problem in the future

as software improves, in fact, some scanning methods already have automated ways to stitch scans. Lastly, special markers could be used, which allow software to know that the object has moved by tracking them. This method relies heavily on software but can make laser triangulation or structured light scanning much more appealing options for scanning people, since their main downside would be largely negated. One might expect long marker placement time, but this can be mostly eliminated by utilising sleeves or suits with pre-placed markers.

Regarding scanning of people, there are three types of scanners that can be distinguished in terms of their mobility, size and covered surface area in a certain amount of time (see Fig. 3). These can be named as stationary, handheld and mini scanners, each differing in scope, use case and price [9]. Stationary scanners are bulky, involve large, almost industrial grade setups where there could be a platform for the person to stand on, either surrounding them with multiple scanners or rotating the platform, or the scanner to get a full scan. Handheld scanners are cheaper than stationary ones simply due to being smaller in scale and scope, they are usually light, close to 1 kg of mass, which allows for good manoeuvrability around the scan subject, but usually cover a smaller area, forcing movement to cover more surface. Mini scanners are lightweight and significantly cheaper than the other two options, but usually cover even less surface area and suffer from low resolution scanning, which can make them unusable in clinical settings for human scanning, although computer algorithms used along multiple mini scanners has some potential in solving this.

Fig. 3. Examples of Three Types of 3D Scanners in Terms of Their Scale [9].
Stationary (a), handheld (b) and mini scanners (c)

For this work, scanning of people will be segregated into two categories: full-body scanning and limb scanning (face or specific area scanning can also be included). Out of the two, full-body scanning is significantly more challenging due to the problems mentioned before. Although there are several sophisticated scanning systems for full-body human scanning, they are prohibitively expensive, with some selling for up to €220,000 [9]. The cost of these systems is likely the reason for them not being widely used and has led to multiple cases of research in developing minimal, low-cost systems for full body scanning [13, 14, 14]. These works all faced the issue discussed before – difficulty of

keeping a person still during the scan. They also all faced the problem of post-processing work, with resulting scans needing significant cleanup. Other research explored mobile scanning applications and their efficacy, which is not only an effort to reduce costs, but also improve accessibility [1, 9, 15]. Recent advancements have allowed for the creation of smartphone applications that can estimate 3D models from pictures. They are a novel way to get a 3D scan easily and cheaply, but they have some recurring issues. There is a lack of standardisation in these kinds of measurements, so it is hard to compare results between different apps and research works on them [1, 9]. Lighting and environmental conditions can also adversely affect results, as found in some studies [15]. Furthermore, for the scan to work, pictures from different angles have to be taken. This means that if the person moves significantly between them, accuracy is reduced with scans failing completely in some cases. Due to these difficulties and other practical limitations, in this work, the focus will be on limb scanning.

Table 1. Summary Table of Referenced Studies in 3D Scanning of Humans

Study	Key words	Conclusions	Difficulties
[1]	Mobile scanning, apparel.	Mobile apps for scanning are sufficient for clothing measurements.	Accuracy varies between devices, environment can affect results, lack of standardization.
[6]	Healthcare, orthopaedics.	Custom hip braces significantly reduce hip displacement progression.	Scanner use in clinical settings is a little impractical, scanning prone patients requires the stitching of two scans.
[9]	Body measurements.	3D scanning is much better than traditional measurement methods, reviewed different scanners, mobile scanning applications.	Inconsistency in scanning protocols, standardized procedures across various industries, particularly when comparing large datasets.
[11]	Healthcare, motor impairment.	3D scanning is effective for body measurement of impaired people, allowing for custom assistive devices.	Involuntary movements can cause problems during scanning, scan stitching and fixing needed.
[12]	Health, apparel, sports.	Digital avatars can be created and used for measurements, personalized health tracking, retail uses.	Movement during scanning, body position variance gives inconsistent results.
[13]	Body scanning, photogrammetry.	Despite using 100 cameras, such a setup can be quite cheap and effective, with an accuracy of around 1 mm.	This many cameras means complex set-up procedure and calibration, synchronization issues, movement during scan.
[14]	Photogrammetry, mechatronics.	Developed an automated photogrammetry system with an accuracy of around 1-2 mm.	Integration of mechanical and electronic components, ensuring good lighting and restricting body movement.
[15]	Orthodontics, facial scanning, photogrammetry	Tested three different scanning systems for facial scans, all stayed below 0.5 mm accuracy.	Movement in between pictures and lighting conditions affecting scan results, differences in detail of capture devices.

1.2. Applications for Limb Scanning

Specifically, the 3D scanning of limbs will be the main focus of this study, due to various advantages that such focus brings. Namely, scan parameters can be evaluated much more reliably and precisely, allowing to optimise them much further than a full-body scan could allow for. Another advantage is that a smaller scale scanner can be used, with less total area needing to be covered. Also, many of the most prominent applications involve limb scanning specifically. Prosthetic sockets, orthoses, orthopaedic footwear all benefit greatly from such scans and do not require full-body dimensions. In

fact, the focus on a limb allows for greater accuracy than normal which is desirable in such use cases. Scanning of a particular area such as the face can also be categorised similarly, since they share more similarities with limb scanning than that of full-body scanning. Repeatability is also increased, since scans can then be made with less chance of movement (in cases of support use) and overall, less volume is being scanned which naturally results in more consistency. Finally, the focus on a specific part allows for more controlled tests, which makes research faster and more reliable.

In full body scanning, it was already discussed that there are challenges like motion during scanning, a large amount of data and difficulty in attaining high resolutions. When focusing specifically on limbs, some of the challenges are alleviated. The data quantity becomes much lower, as the focus is on an over 5 times lower surface area of the body. Higher resolutions are also easier to achieve due to this surface area reduction. However, the biggest difficulty remains – patient movement during scans, which is in fact even more pronounced when focusing on specific limbs. This is due to the way that they need to be scanned – they either need to be rotated 180 degrees after scanning one side or to be scanned while the scanner is being continuously moved around it. The latter would require a more compact scanner that could be more easily manoeuvred. Such new challenges may cause incomplete or poor results, with models containing floating artefacts, missing parts of the surface and lost detail. Scanning time will also remain quite lengthy because of the factors explained already, although shorter than for a full-body scan.

Motion is generally where most limb scans go wrong, and the analysed papers describe three ways to deal with these issues. The first is a passive support, such as braces, vacuum bags, or simply see-through objects like simple glass boxes, resting on a surface reduces limb movement significantly. One study showed that this can be effective, keeping stump error under 0.3 mm but can be uncomfortable for the patient after a couple of minutes [19]. The second method is to use tracking markers or SLAM (simultaneous localisation and mapping) targets so that the software can realign frames even if the limb shifts, although this will not work if joint angle changes. A study that used this cut drift almost in half with a small set of optical markers, though the setup took longer [22]. The third method is to simply fix the broken data using computer algorithms tailored to this, such as in one study, where hand-scan error was reduced from 1.2 mm to 0.5 mm after some heavy processing [17]. Finally most multi-camera photogrammetry rigs bypass this issue altogether by capturing a scan within less than a second, during which movement is not possible.

Some considerations also need to be made regarding software and post-processing when switching to limb scanning. In full body scanning, the finer details like ears, toes or fingers are not the main focus and so it can be acceptable for them to lose accuracy. Those kinds of minute details are much more important when focusing on a limb, though. Even when scanning a much smaller area, it can still be hard to capture finger, toe and ear measurements correctly and these details usually end up damaged or distorted in some way (see Fig. 4**.** Example of Damaged Leg Scans [20]). This means that post-processing work is unavoidable in most cases. The kind of work done and software used depends on the specifics of each scan, things like the type of scanner used, the kind of body part scanned and resulting scan quality all contribute to this. Sometimes, scans need to be stitched together if the process is done in two passes [6]. Missing surface area can be filled in using automatic tools that connect points of a hole either directly or tangentially. In rare cases, manual reconstruction of some features is needed, where existing points have to be connected one by one or new points have to be made.

Fig. 4. Example of Damaged Leg Scans [20]

Over the last couple of years, 3D scanning has been making great strides of improvement. Scanners are lighter, smaller and cheaper, all while increasing the captured resolution and scan speed. In this aspect, the development of this sector is similar to AI, where in a couple of years the whole field is expected to be different. This can be seen in recent works, where mobile scanning achieves similar results to traditional scanning methods [15]. It should be taken with a grain of salt, though, as the scanning was of the face, which does not involve some of the challenges of limb scanning. Other studies showed that measurements can be captured quickly with high accuracy [1]. This advancement speed means that studies become less relevant very quickly, which is something of importance to note.

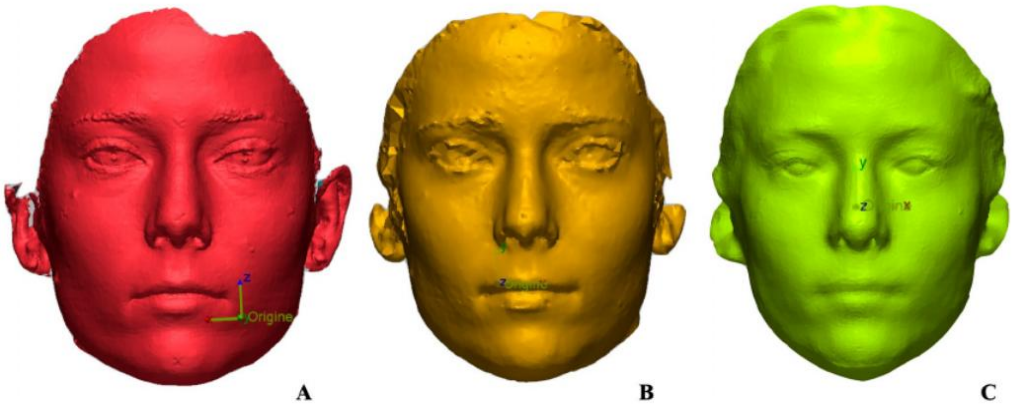

Fig. 5. Face Scans With 3 Different Scanning Methods [15].
A – structured light, B – photogrammetry, C – mobile application

Some of the most important parts of scanning limbs are the decisions made regarding methodology, which is more intricate when dealing with time of flight, structured light and laser triangulation scanners. For these methods, decisions involving scanning protocol must be made, such as: whether the limb will be immobilised and captured through multiple, overlapping passes of both sides, or whether a continuous circular sweep of the scanner will be employed. Scanning each side of the limb consecutively is the simpler of the two, since this allows the limb to be rested on a surface, significantly reducing motion. Continuous scanning often times requires the limb to be suspended in

air, which leaves it suspect to more unintentional oscillatory movement, making it more challenging. There is no clear winner, however, and the method should be chosen based on the type of scanner used and the specifics of each use case. In some studies, these problems are omitted entirely, which can be accomplished through scanning of a 3D printed copy of a limb instead of a real one, eliminating potential discrepancies due to movement during data acquisition [8]. In another work, researchers chose to use two scanners instead to simultaneously scan both sides of an arm [17]. This is a novel approach, but has a difficult calibration process, since both scanners need to be synced perfectly for it to work.

Fig. 6. Example of a Scanning System Where an Arm is Scanned from Both Sides Simultaneously [17]

There are also some differences in scanning legs as compared to arms. In general, legs are easier to scan, since they can simply be scanned while a person is standing, but this does not allow for complete foot capture, as the sole is not incorporated. In order to get a complete scan of the foot, things get more complicated, since the average person cannot hold their leg up for any considerable amount of time to allow scanning. Some studies solve this by placing the foot on a glass box, which is effectively invisible to a laser scanner [19]. Another way to go about it is to use some supports that could keep the limb in place [20]. Using supports has the downside of not getting data from the parts of the limb that are touching them. The only way to solve this is to do scan stitching after scanning each side separately.

One seemingly underexplored area is the automation of limb scanning, while one study did use some kind of automated scanning procedure, it was not the focus of the study and so it was not discussed [21]. Automation of hand-held scanning could be done with a robot arm, greatly enhancing the process. Robotic scanners are already used widely in manufacturing for quality control and should be relatively easy to implement for human limb scanning. Using such a method, the inaccuracies caused by human error would be mostly eliminated, ensuring that different scans are always analogous to each other, which also allows for more reliable comparison of results. Furthermore, this would be able to push the respective scanner to its limits, since an automated process can ensure an optimal motion path of the scanner, maximizing quality of results. These factors would also push scan speeds to the highest possible, since there would be no errors that occur due to suboptimal scanning distance or incorrect speed and no backtracking would be necessary. To that end, in this work we will automate scanning via robot arm and test whether this has any significant effect on results. This also involves finding best scanning speeds, average error values among other parameters.

Overall, many works have been published within the last 5 years that focus on human limb scanning, showing the relevance of this field. A lot of different approaches have been tried, but in general, it

seems like structured light scanning retains the highest scan quality to scan speed ratio. Some of the studies referenced before have had some meaningful results from scanning, below is a table summarizing data acquisition time and average error that they achieved, as well as some additional notes about them (see Table 2).

Table 2. Comparison of Human Face/Limb 3D Scanning Studies

Study	Target region	Acquisition time	Average error	Additional notes
[16]	Face	< 5 s	3.8-6 mm	Direct comparison with manual anthropometric measurements.
[15]	Face	2-4 s	< 6 mm	Multi-angle capture reduces motion artifacts.
[18]	Face	1.5 ms	3–4 mm	Emphasis on calibration and reliability in less controlled settings.
[17]	Hand	8.9 s	2.5 mm	Scanned from both sides simultaneously instead of moving around the arm.
[8]	Hand	< 2 s	2.5-4 mm	Used a 3D printed hand instead of a real one.
[10]	Hand	~90 s	0.6 mm	50 cameras used, cost below €1,000 achieved a good surface area coverage of 96 %.
[19]	Leg/Foot	60-90 s	-	Used markers, scanned the leg by placing it on a glass box.
[20]	Leg/Foot	26-48 s	-	All scanners used had a similar data acquisition speed that was much higher than plaster casting.
[21]	Arm/Stump	< 5 min.	0.25-1 mm	Used an iterative closest point algorithm to improve the result.
[22]	Arm/Stump	~5 min.	0.3-0.4 mm	The patient's arm was held by a caregiver.

A prediction for the future is that this field is bound to explode in popularity as digitalisation of all sorts of services continues, eventually scanning of the human body will become a common occurrence in ways that were not expected yet either. Once the technology becomes available enough and easy to use, it will appear everywhere from sports and fitness to the apparel industry, a visit to a gym could start with a body scan to measure muscle volume of certain muscle groups, while a visit to a clothing store could entail digitalised fitting rooms, where body measurements are taken via a quick scan.

1.3. Chapter Summary

To sum it all up, the use of 3D scanning solutions for human anthropometric data acquisition is abundant in recent literature. Clear improvement can be seen year by year and shows the kind of solutions that are out there. While mobile applications have increasing interest, showing promise for photogrammetry, it still lags behind structured light and laser triangulation scanning in terms of accuracy and detail retainment. Scientific works showed that scanning time can range from a few seconds to 5 minutes, depending on the desired resolution, chosen method or complicating circumstances. It was also found that overcoming the challenge of movement during scanning is an ongoing problem. Some researchers opted to mitigate this by placing the limb on supports, which caused some parts of the scan to require clean-up. Others chose to speed up scanning time, either by using faster scanning methods or even using multiple scanners to cover all angles at once. Generally, there is no clear-cut solution that would be the best. No works focused on automating the scanning process, showing an underexplored niche in this topic.

2. Relevant Theory Regarding 3D Scanning Technologies and Chosen Solutions

2.1. Explanation of Surrounding Theory

In the 3D scanning field, there are four distinct technologies that could be used to scan humans: laser triangulation, structured light, time of flight and photogrammetry. It is important to discuss these methods before choosing one for this work, as each of them have their own strengths and weaknesses. As explored previously, authors of similar works tend to either focus on one method or test and compare several different ones, in this case, we want to focus on one due to the limited resources and scope of this work. Below is a bit of background information about each technology that is viable for human scanning, with explanations of the final choice.

One of the most prominent 3D scanning implementations today is laser triangulation. With it first starting to be used in the 1980s, it is still widely used in manufacturing for quality control, reverse engineering of parts and so on. The main principle behind this technology has been explored for hundreds of years and has to do trigonometry. This is based on the idea that distance to the object can be calculated if the distance between two other points in the triangle are known, as well as two other angles. In laser triangulation 3D scanning, this principle is used to calculate how far the object is from the laser. Since the distance between the laser and camera is already known during calibration and we also know the laser angle of incidence, while the second angle is determined by the laser dot's position in the camera's image. Emission of the laser is either in the form of a line or some simple pattern, where each part's position can be triangulated. The rest is handled in software through intensive computation, mapping out each measured point on a point cloud. One issue with such a method is that when multiple scans are taken from different angles, they have to be merged which can be challenging. However. software is well developed for this technology and automates most of the process, significantly mitigating the issue. Residual error is mostly dominated by incorrect calibration of the camera and laser source.

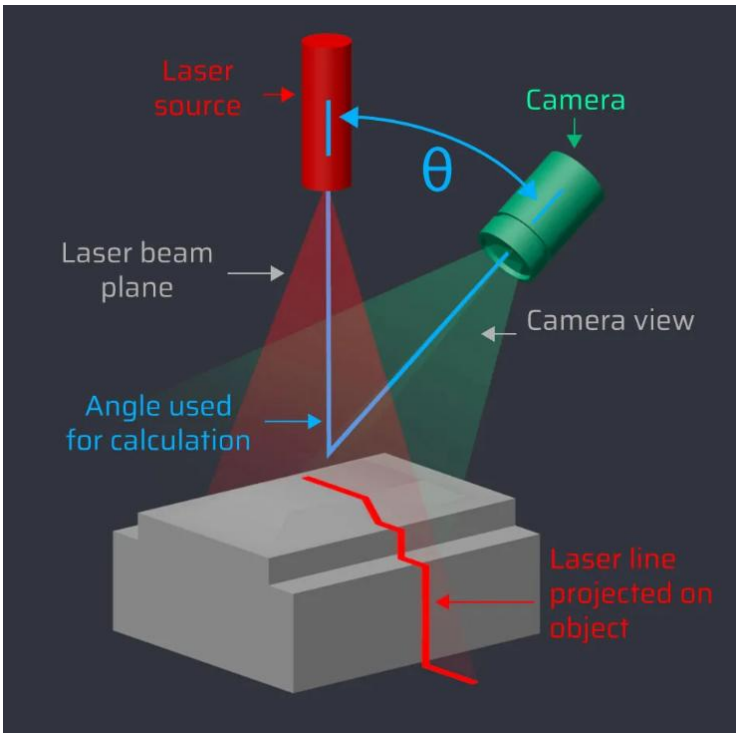

Fig. 7. Principle of Triangulation [23]

Another method, which is very similar in concept to laser triangulation is structured light scanning. This relies on essentially the same principle of triangulation, but instead of tracking a laser point, or a line of many points, the camera captures an entire projection. It works because when combining a camera and software, the distorted projected pattern can be analysed. This allows for less precision but is generally faster and can cover a wider area than the laser variant. It was in fact tested before laser triangulation despite being more complicated, due to laser technology being rather underdeveloped at the time. Generally, it is easier to use than the laser version but is less precise and more sensitive to poor lighting conditions. Results can also vary with different skin colour and glossiness, as dark or shiny surfaces can drop signal to noise ratio by 30% or more. It is also safer to use on humans for example due to the use of LED projectors IEC class 1, relevant since some lasers can be dangerous to the eyes, but for limb scanning this is not a key problem.

Time of flight is yet another method used for obtaining 3D measurements. It works by simply measuring the time taken for a beam of light to travel to the object and return back to the sensors. This method allows for much wider area coverage and from significantly further away, with some advanced applications allowing to capture landscapes of multiple square kilometres. Due to this advantage, it is often in military applications or architecture and construction. Since the technology is relatively simple, it has been implemented in mobile phones, such as Apple's iPhone 12 pro and later versions. These implementations have been tested in scientific literature and show promise, proving they could be used to scan people [24]. The only downside is the limited resolution of the scan, with deviation varying from 0.16 mm to 0.35 mm depending on colours and lighting, found in the study. Overall, the mobile version of the technology was deemed unsuitable for small object scanning, which is undesirable for more localized uses like limb scanning.

The final method to be considered is photogrammetry, which is a method that uses software to obtain 3D data from pictures. Pictures are usually taken from multiple angles, which allows to find 3D data from them. The process works something like this: computer software detects common features between multiple images, this is used to find the relative camera position of each picture, then stereo matching is used to find matching pixels between the pictures and triangulate point positions, generating a point cloud. Using pictures has the advantage of capturing measurements almost instantly, this however requires multiple cameras. This means they need to be synchronized, which can be a difficult process. Using such a method and trying to achieve high resolution can get very expensive. Another problem with this method is the post-processing time. Depending on the resolution of cameras used and the number of pictures taken, for an average computer, algorithms can take up to several hours to compute the 3D point cloud [14]. Generally, this technology has potential for human body measurements due to how fast the scan can be done, essentially eliminating possible movement during the scan. However, due to the limited resolution of affordable setups, some applications are not possible, for example, clinical precision (errors below 0.5-1 mm) may not be achievable.

An important consideration for these technologies is how safe they are to humans, since the whole essence of this work is to use these for human scanning. In terms of possible harm, only eyesight is of importance, since no other kinds of damage is possible with any of the mentioned methods. The most dangerous to the eyes is laser triangulation, although structured light could also be harmful in some cases, as well as photogrammetry in case camera flashes are used, which can cause eye irritation. Since it was decided that limbs will be scanned, not faces or full bodies, there is no issue with utilising laser triangulation scanning, even though lasers can damage eyesight if directly

exposed. Regardless, it could be an important thing to consider, especially if designing an automated scanning system, eye safety in the form of possibly using some covers that block the patient's view.

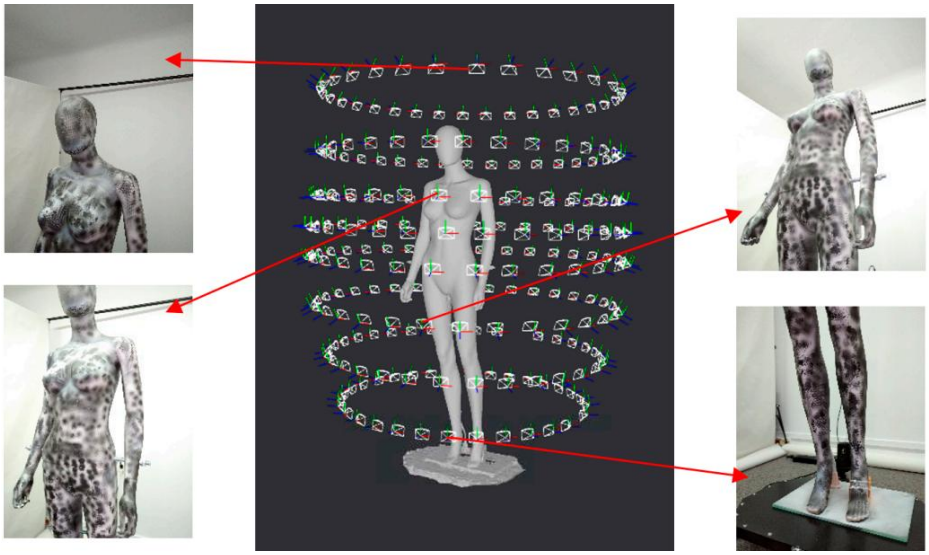

Fig. 8. An Example Photogrammetry Setup [14]

For the purpose of this work, laser triangulation is chosen as it is the most effective in this case. Since the main downside of laser triangulation scanning is the relatively low area coverage, it can still work well for specializing in limb scanning as it is a small enough application for such a method. In addition, due to the nature of this 3D scanning method, automating it should provide the most benefit out of all the discussed technologies, making it a primary target for automation testing. Handheld laser scanners are hard to handle as a constant distance from the object is required for a good scan, as well as constant and continuous movement. Automation via robot arm solves all of these issues and should show better results than doing scans by hand, especially comparing to less experienced users.

Table 3. Applicable 3D Scanning Technologies and Their Capabilities

Technology	**Range**	**Resolution**	**Post-Processing Time**	**Notes**
Laser triangulation	0.1 – 2 m	10 – 50 µm	Under 30 min.	Typically covers up to 1 m^2
Structured light	0.3 – 3 m	0.01 – 0.1 mm	Under 30 min.	Typically covers up to 3 m^2
Time of flight (LIDAR)	1 – 1000+ m	2 – 5 mm (cm at longer ranges)	Under 60 s	Accuracy varies with scan distance significantly, can cover area in the km^2 range
Photogrammetry	<0.1 – 1000+ m	0.5 – 5 mm (accuracy loss at long distances)	Up to several hours	Resolution depends on image quality and number of images; area coverage varies highly but can be very large

In general, 3D scanning technology has advanced significantly in recent years, with current scanners outclassing older ones by leaps and bounds. As a reference, a table is included listing the parameters of 3D scanners released over the last 3 years (see Table 4). These advances mean that some older scanner that might have been tested in other research works are no longer competitive with the market and the data loses some significance. For this reason, this work focuses not on scanner performance

testing, but specifically on the benefits of automation for handheld 3D scanners. This rapid development is largely due to the decreased cost of materials and the addition of AI processing tools, which were majorly improved recently.

Table 4. List of Some 3D Scanners Released by Major Manufacturers in the Last 3 Years

Scanner	**Maximum resolution**	**Data acquisition speed**	**Weight**	**Improvements over predecessor (~5 year gap)**
Artec Leo (2022)	0.2 mm	3,000,000 points/sec	2.6 kg	~2.5x finer detail, 50% faster data acquisition, 2x the computing power, AI processing
Artec Micro II (2023)	0.01 mm	~1,000,000 points/sec	~2 kg	Not available
Shining 3D EinScan HX	0.05 mm	1,200,000 points/sec	710 g	3x higher resolution, 25% lower data acquisition speed, higher area coverage, ~35% lighter
Creaform HandySCAN Elite (2022)	0.025 mm	1,300,000 points/sec	940 g	2x higher resolution, 33% higher accuracy, 2.7x faster
GOM Scan 1 (2022)	0.037 mm	~6,000,000 points/sec	~1.5 kg	20% higher resolution, 3x faster capture, ~3x lighter
Peel 3 (2022)	0.1 mm	550,000 points/sec	950 g	Not available
Polyga H3 (2023)	0.05 mm	~1,500,000 points/sec	2.5 kg	Not available

2.2. Chosen Research Methodology

In this subsection, methodology for this research will be discussed, explaining the steps to be taken, listing the used tools, equipment, software, etc. First of all, situation analysis was done in the form of quantitative and qualitative research of relevant scientific works, which can be found in chapter 1. This was a mixed method due to the incomparability of some research, which focused on different techniques, body parts and measured in different areas. As a result, it was required to not only observe and compare numeric data, but also judge the qualitative part of each work, noting the challenges faced and choices made. This is the basis for the decisions made in methodology of this work.

The goal is to automate 3D scanning of human limbs using a robot arm in order to improve existing scanning practices. Laser triangulation is the method chosen in this work due to the precision it provides, as well as being the most compatible with automation via robot system. To be more precise, the aim is to eliminate human error from the process, test and find the best parameters for scanning. In the analysed studies, none of the authors considered the impact that varying scanner movement speeds and scanning height may have. This could be a major constituent in problems such as fluctuating mean error tolerances seen in some works [13, 16, 17]. When it comes to laser triangulation scanning, there is an ideal distance at which the scan will have optimal results, as mentioned above. This distance is never properly kept when scanning by hand, due to the way human movement is and the uneven nature of limb surface geometry.

The following is the final methodology of this work, chosen based on review of analogous research, including all steps as well as possible variations. First, the arm of a human is scanned and 3D printed

as a reference, this could also be done on a mannequin arm. The scanner used is also scanned by a different scanner, in order to manufacture a replica for safe testing of the robot. Then, a program is set up that will move the robot arm in arcs around the subject to capture the sides as well as the top. Afterwards, the scanner is attached to the robot arm using a custom-designed mount. The next step is to scan the 3D printed or mannequin arm and scan it using the robot, in two passes. First pass captures one side, then the arm is flipped lengthwise, and the other side is scanned with the second pass. Thereafter, scan data is post-processed using specialized software, scan stitching will likely be needed, which could cause accuracy discrepancies. Finally, scans are compared between each other, noting the differences in data size. They can then also be compared to the STL (stereolithography file) model of the 3D printed arm, which would allow to judge the accuracy. This summarized methodology is also provided in the form of a flowchart in the figure below (see Fig. 9).

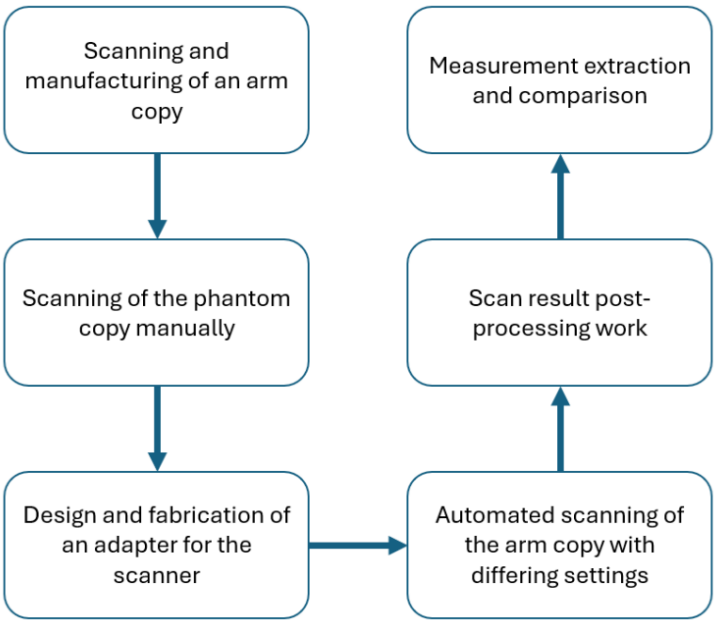

Fig. 9. Flowchart of the Methodology for Scanning

In this work, the software tools to be used are as follows: Autodesk Meshmixer, used for cutting edge mesh editing and manipulation; Dassault Systemes Solidworks, used for 3D modelling of the scanner to robot arm adapter; Creaform VXelements 12 software, used for initial post-processing of scans to remove outliers, reduce mesh density and evaluate standard deviation of the surface; Microsoft VisualStudio, used for modifying robot arm code; ABB RobotStudio 2025, used to send commands to the robot as well as view simulations of the robot, testing the code risk-free. The main scanner which will be used in the work is Creaform's Handyscan 700. It was chosen due to being suitable for this application and its widespread use in other works as well as generally good user reception. Specifications are resolution – up to 0.05 mm, capture speed – 480 000 measurements per second, capture area – 275 x 250 mm, ideal distance to object – 300 to 450 mm, weighing 0.85 kg. While recent scanners have significantly better capabilities, this scanner is sufficient to test the benefits of automation and find best parameters. The chosen robot arm is ABB IRB 1200, which can move a payload of up to 7 kg in 6 axes of motion, with a repeatability of +-0.01 mm at a speed of at least 250 °/s. An issue that is apparent with the chosen robot is that it does not support large enough range of motion to complete 360° scans, mainly due to the requirement of keeping the scanner at the ideal

distance window of 300-450 mm. The way this will be solved is by scanning the top and bottom of the subject separately, later merging the two scans in the scanner software VXelements 12.

Fig. 10. Hardware Used in the Work.
Left image – robot arm ABB IRB 1200, right – scanner Creaform HandyScan 700

In the first step of manufacturing a replica of an arm, a mannequin arm could be used instead due to the possibility of movement, even when supported. Motion during scan would obviously be a problem, especially when intending to compare scan results with different settings. A static arm fixes this issue, which will allow to optimize scanning settings before scanning a real arm. The ideal way to do it would be to scan an arm with a handheld scanner, then manufacture a copy of that arm using fused filament fabrication. The mannequin arm could also be held by a person during a scan, which would simulate the unstable nature of scanning someone's arm, this still holds an advantage as there is no possible discrepancy (such as changed joint angles) between 3D printed copy and the real arm in this case.

The robot arm will be programmed using the language used by its manufacturer, called "RAPID". Trajectory to be tested is a slightly complex one that resembles a half-circle, with some variance in distance from scanner to subject. These will then be run using several different speed profiles to determine the effect of movement speed on scan quality and amount of data retrieved, as well as quality of such data. In all test cases, two scans will be required in order to capture both sides of the arm. In further steps, an adapter allowing the use of HandyScan 700 on the robot arm ABB IRB 1200 will be designed using the scanned scanner's model and physical measurements of the robot arm.

After retrieving scan results, some post-processing will be done to ensure scan comparability and remove any potential problematic areas. Scan stitching will be employed to combine scans of different sides of the arm together, which is necessary in order to attain full volume data. Some open-source algorithms could be used in order to filter out bad data points, but in this case the likely solution will be to simply use the built-in tools of VXelements software. Then, scan results will be compared, evaluating the difference between scan speeds and distance to subject. A huge focus will be the amount of data extracted and qualitative evaluation of each scan. Since the arm being scanned will

be 3D printed, accuracy can be easily compared between the base model and the scanning results. The effects of scan stitching on accuracy should also be evaluated.

As a final methodology, it was decided to hold five total experiments, all of which follow a similar approach to what is described above. One is set to focus on the effects of laser exposure time for two different surface finishes, a glossy, lighter surface and a matte, slightly darker but still light surface, which will be attained by spraying a primer on the manufactured arm replica. In another experiment, scan reproducibility will be tried in an attempt to find scanner noise and how stable the results are. The third experiment will be the biggest one in scope, testing various different resolutions at varying speeds in order to determine the optimal combination of speed and resolution. This will likely still be subjective depending on the desired use case, so results will be provided more as recommended ranges rather than a concrete best value. In further tests, users of two different skill levels will be compared to the robot arm, on criteria such as scan completeness, scan quality and scan time in order to find whether the scanning path is relevant to each metric. Finally, the entire system will be put to the test by attempting to scan a real person's arm, using the optimal settings found, insights on automated setup quality should be acquired.

2.3. Chapter Summary

To conclude the chapter, multiple choices for 3D scanning technology were considered. Including photogrammetry, time-of-flight (LIDAR), structured light and laser triangulation scanning. Based on existing literature and general context of this work, a laser triangulation-based scanner was chosen for the automation testing. The general outline of the methodology was also explained along with the tools, software and hardware used. Robotic arm ABB IRB 1200 and portable scanner Creaform HandyScan 700 were both chosen as suitable for use. Methodology was described in 5 main steps: scanning and manufacturing of a copy of a human arm; scanning of the arm copy by hand; fabrication of an adapter for the scanner-robot connection; automated scanning of the arm copy; post-processing; result comparison.

3. Project Results and Implemented Solutions

3.1. Explanation of Implemented Solutions

The first step in the practical part is to obtain an STL mesh of the scanner Creaform HandyScan 700, which was done by scanning it using a different scanner. The resulting mesh needed extensive post-processing work, although VXelements (scanner's software) has some automated mesh enhancement capabilities, applied when finishing a scan, these were not remotely enough. The repair was conducted in Autodesk Fusion, which is much better suited for such work with features such as background removal, hole filling, sharp edge softening and mesh decimation. Utilising said features, the mesh was repaired after a lengthy process, and the result was a watertight mesh made up of 7,436 triangles, ready for fused filament fabrication (FFF). With this model we can now accurately manufacture a replica using FFF via a standard, consumer grade 3D printer. The copy was made using white polylactic acid (PLA) material, with a layer height of 0.1 mm, nozzle diameter of 0.6 mm, the result, along with the mesh images are visualised below (see Fig. 11). Having a replica on hand allowed for more rapid testing of robot parameters, experimental setup and program code, ensuring that no collisions occur which could damage the scanner.

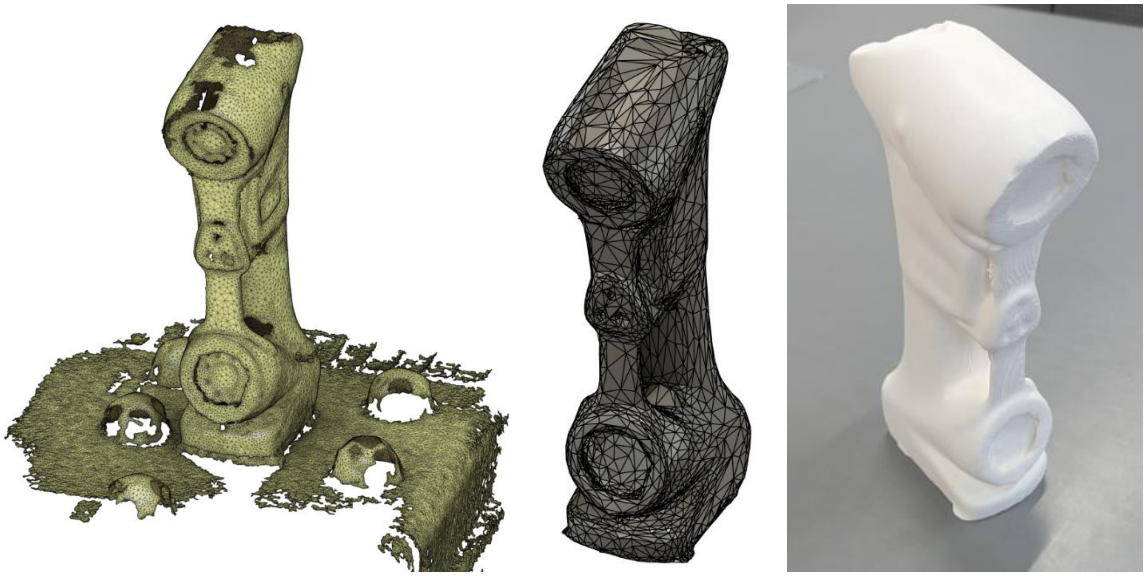

Fig. 11. Scanner Replica Production Progression Images.
Left image – raw scan mesh; middle – STL model of the scanner, containing 7436 triangles; right – 3D printed copy

As mentioned in the previous section, testing of scanning parameters is not viable using a real person's arm, which means a static copy is needed, which can also be manufactured using FFF (fused filament fabrication) and to do this, a high-quality mesh is required. The plan was to scan an arm of a volunteer manually, using the hand-held scanner, but this was a tedious and error-prone process, resulting in models that had many problems: holes, missing surface area, artefacts and rough patches (one example in Fig. 12). After at least 10 attempts, a sufficiently high-quality model was obtained (evaluated qualitatively), this mesh could be mostly repaired using Meshmixer software. Below is the resulting model (see Fig. 13) visualised, showing it before post-processing and after. Overall, these scans made even more apparent the possible issues that can occur during scanning, especially that of fine details like fingers. Since post-processing work was done, the model is no longer true to reality,

this is acceptable since it will be used to manufacture a replica for scanning, not for directly measuring the person's arm.

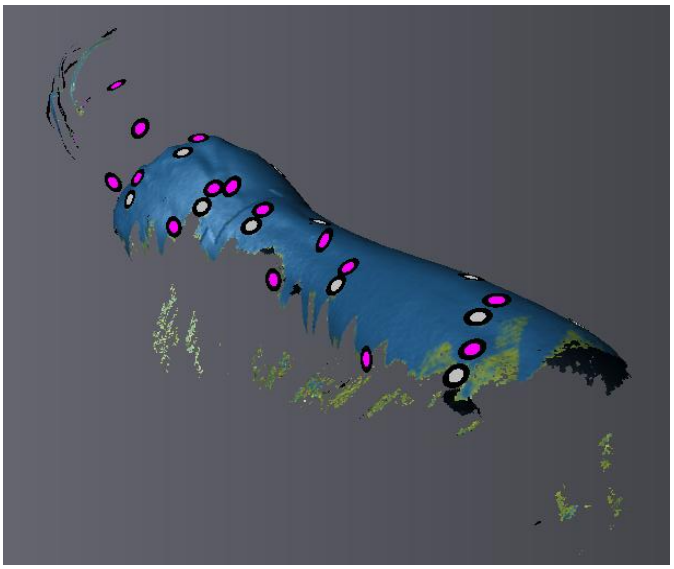

Fig. 12. Failed Scan Mesh Due to Scanner Error, Lost Track of the Targets Due to Subject Movement

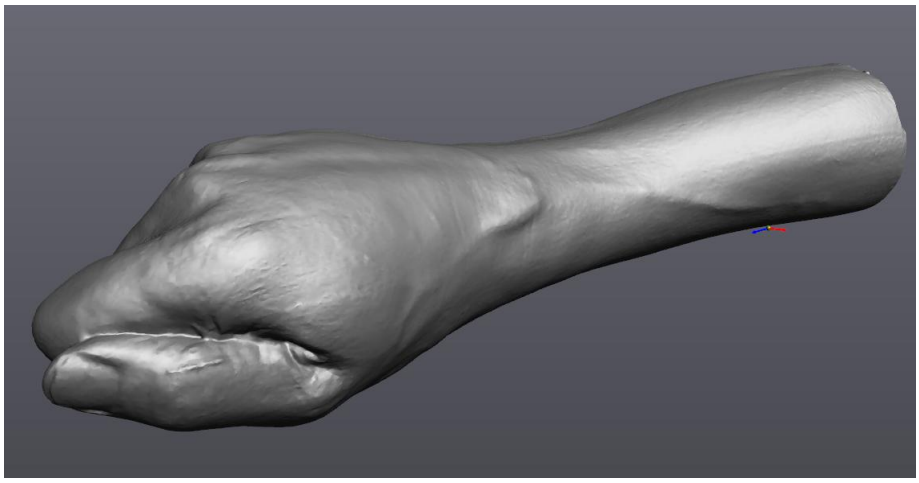

Fig. 13. Nominal Hand Mesh After Post-Processing

Afterwards, an adapter had to be fabricated to allow the scanner to be mounted on the robot arm. It was modelled entirely manually by importing the 3D scanner's mesh in SolidWorks software and tracing the outlines at cross-sections in two different locations of the part meant for holding. The two outlines are then used to create a solid loft, which can then be easily used to model the rest of the adapter. Since the scanner does not weigh much (<1 kg), no static simulations were conducted to verify adapter strength and it was simply made thicker than normal, at 10 mm thickness. In this design, the adapter is made of two parts that are secured via bolts which allows for easy mounting. A gap is left between the top connection of the parts to allow for leeway in tightness and allow for an imperfect fit, as well as to tighten the scanner more securely. This was then 3D printed using PLA with a layer thickness of 0.1 mm and nozzle diameter of 0.6 mm (Fig. 14). Manufacturing was a success, and the adapter was able to be attached to the robot arm with no problems, enabling the fastening of scanner to robot toolhead. It is attached to the toolhead using 4xM5 bolts of 10 mm length and the second part that secures the scanner is mounted with 30 mm length, 4xM5 bolts and nuts.

Fig. 14. 3D Model of the Adapter

Once the adapter was ready, it was possible to effectively prepare robot code with the mounted replica of the scanner acting as a safety test for collisions. The logic of the code was prepared in Microsoft Visual Studio Code and then tested by running simulations of the robot arm on ABB RobotStudio 2025 software. RobotStudio allows for reliable and accurate simulation, since the company developing it is also the manufacturer of the robot arm. First, ABB IRB 1200 robotic arm is imported into the workspace, followed by already attained models of the scanner, scanner‘s adapter and copy of the human arm (see Fig. 15). In this workspace there are three ways to give instructions to the robot: create target points for the robot to follow by moving it to them, giving a 3D path for the toolhead to follow, or instructing coordinate-based movement via code. For the desired robot motion, only programming is a viable option, since it allows for much more precise control of the path and is much easier to modify and adapt. In the RobotStudio workspace, all coordinates given are referenced from the base of the robot arm, so the zero point is there and any position referenced from here on out will be measured from it. A starting point for the toolhead is chosen as [350, 0, 750] mm, and the hand model is placed at [340, 0, 220] mm.

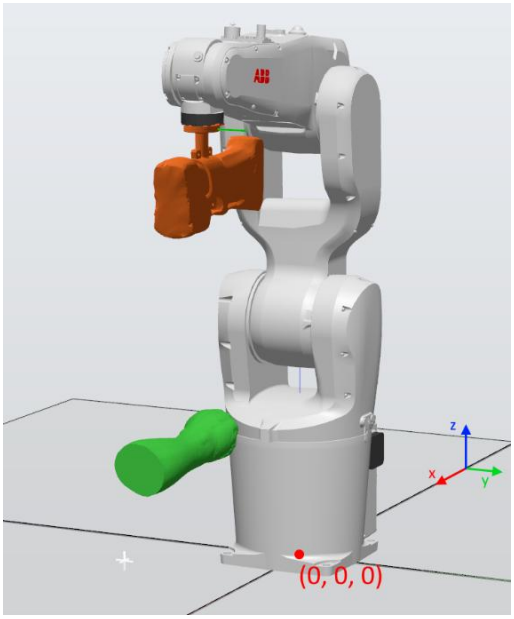

Fig. 15. RobotStudio 2025 Workspace with the Full Setup, Zero Point and Coordinate Axis

3.1.1. Robot Programming

In this work, it was opted to only scan one side of the arm at a time and when a full model is desired, scan both sides separately and then stitch them together. This decision was made due to the limitations of the robot arm ABB IRB 1200, which simply does not have the degrees of freedom needed to complete a 360° scan. What it also means is that tests with a real hand won't be the focus of this work, since the main failure point for a real arm is subtle joint angle changes, which will prohibit scan stitching from being feasible should that occur.

The robot arm was programmed using ABB group's high-level programming language, called "RAPID", which was developed specifically for their robots. The purpose of the code, as already discussed, is this: move the robot in half-circles around the human arm in several passes while the toolhead faces it. The angular movement was instructed using the "MoveC" command, which is used to move the toolhead circularly to a given destination. Each "MoveC" call requires two points on the desired circle and at least two calls are needed for a circle, which means these points must split the circle into quarters, to avoid moving in an ellipse shape instead. In the main code, there are five points that are generated using trigonometry (see Eq. 1 11111below), one extra duplicate is needed in case a new arc is drawn without the robot moving, which would cause an error if it were the same point that it is already in. To make the toolhead always point towards the circle's centre, an angle ϕ is computed using the atan2 function, the angle is then used to get an orientation quaternion using the "orientZYX" function. The exact path that the robot head takes is visualised below, drawn in the simulation software (see Fig. 16).

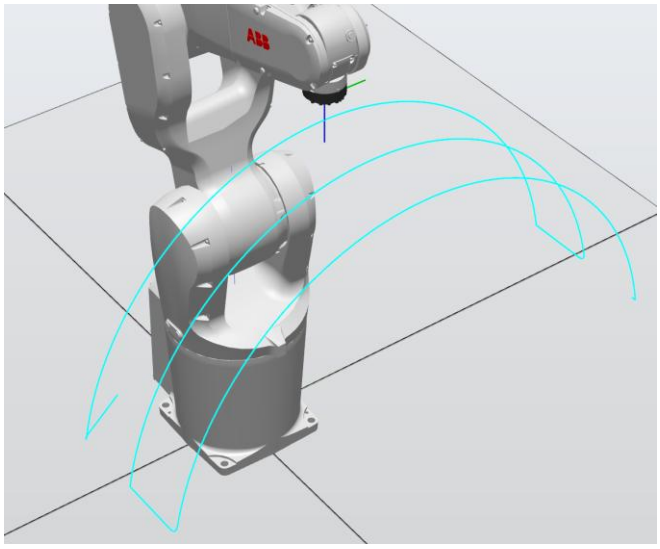

Fig. 16. Robot Toolhead Path Visualised in RobotStudio

During testing, better results were received when also orienting the toolhead slightly tilted forward, which allowed for capture of the front of the hand, this was implemented through a second angle ϕ_2 in similar fashion. Main variables that are in the code: x0, y0, z0 – coordinates of the circle center, b – radius increment per step (in case we want to change radius every arc), Rmax – maximum radius, r1 – tracks current radius, Rmin – minimum radius, started – tracks whether the robot was positioned already, speed – sets robot speed to a preset. First if statement moves the robot to the starting point if this was not done already, second condition checks if we are not at the minimum radius and runs the main code logic of robot movement described before, lastly the robot is moved back to the starting

point. After experimentation with various paths, the overall best performing one was chosen to be used in further tests. This best path involves three half-circle movements, with a forward motion of 120 mm in the X axis in between them. To make it easier to comprehend, the code is visualised in a logic chart schematic below (see Fig. 17), find the full code in Appendix 1.

$$y_1 = r \cdot \sin\left(-\frac{\pi}{2}\right) + y_0, \quad z_1 = r \cdot \cos\left(-\frac{\pi}{2}\right) + z_0, \tag{1}$$

$$y_2 = \frac{5r}{6} \cdot \sin(0) + y_0, \quad z_2 = \frac{5r}{6} \cdot \cos(0) + z_0,$$

$$y_3 = r \cdot \sin\left(\frac{\pi}{2}\right) + y_0, \quad z_3 = r \cdot \cos\left(\frac{\pi}{2}\right) + z_0,$$

$$y_4 = y_2, \;\; z_4 = z_2, \;\; y_5 = y_1, \;\; z_5 = z_1.$$

where: y_1, …, y_5 are the Y coordinates in the world frame (mm); z_1, …, z_5 are the Z coordinates (mm); r is the current radius (mm); y_0, z_0 are the circle's center coordinates (mm). 5/6 of the radius is applied on the half-circle's top point because the hand replica is located slightly below the circle center, this ratio ensures that the same distance is kept more or less at all points in the path regardless of that.

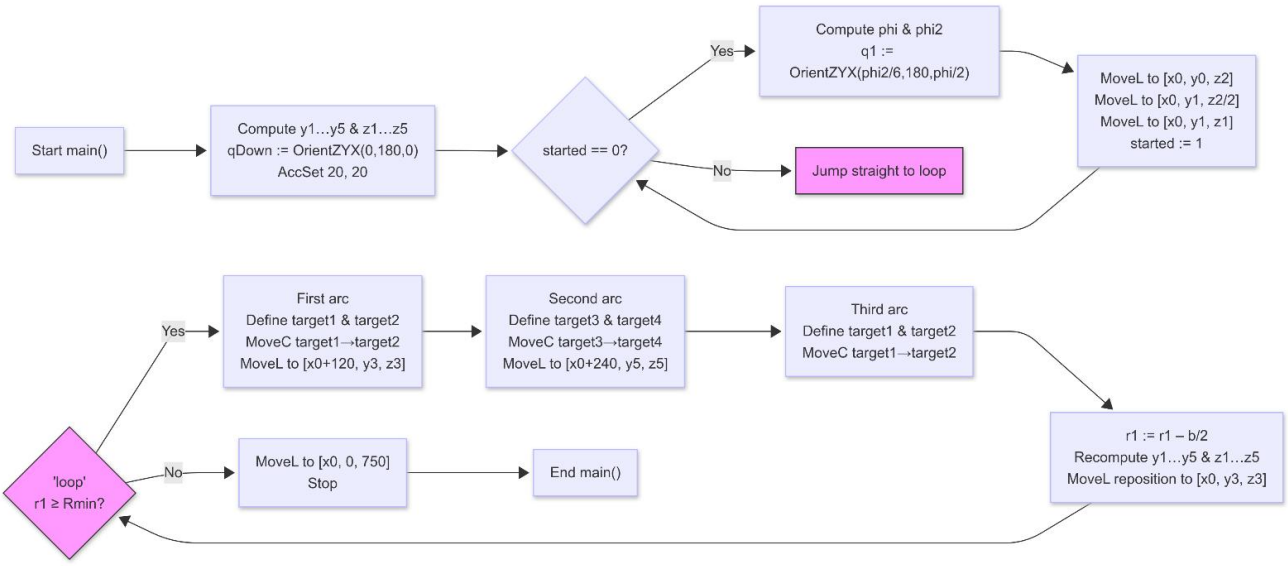

Fig. 17. Code Logic Flow Chart

3.1.2. Experimental Setup and Measurement Explanation

The very first step is to prepare the scanning subject (3D printed arm) for scanning, which consists of FFF support removal, light polishing of rough areas and placement of 3D scanning markers, referred to in software as targets. As a guideline, the markers should usually be placed 10 cm apart for purely flat parts. In this case, the shape is complex with many curves, which is much closer to a cylinder, than a flat plane and requires denser marker placement. These markers were placed more generously in areas where the surface has a sudden change in angle (sharper corners), such as knuckles, other areas around the fist and less so in places where the surface is constant, such as the forearm. This resulted in a total of 40 markers applied to this subject, none of which were placed at the base of the arm (flat part), since it was decided that there is no need to scan that area as it would not be assessed.

Following up is the preparation of the experimental setup environment, which includes positioning of all integral parts, support placement and scanner attachment to the robot arm. The scanner is oriented so that the cables are in front of the robot to avoid any potential collisions when the toolhead is pushed to its maximum angles. On the table where robot is attached also sits a metal tooling plate of 60 mm height, although it will not be used for attaching anything and simply serves as a solid base and height addition. This surface also needs markers to be placed so the scanner can orient better and reduce possible errors during the scan, as a result – 30 markers are placed in 5 columns of 6, about 70 mm apart. Transparent supports are chosen for the 3D printed arm, which fit well in this use case as they are virtually invisible to the scanner. They have a height of 160 mm and are placed on the global X axis, 150 mm apart where the first support is at [430, 0, 60] mm from the base of the robot arm (treated as the zero point still). Finally, the 3D printed arm copy is placed on top of the supports, with its middle point located at [550, 0, 240] mm in global coordinates. Safe use of the robot arm was followed according to manufacturer instructions (product specification manual – IRB 1200) provided online [25], which were also used to prepare the robot for work.

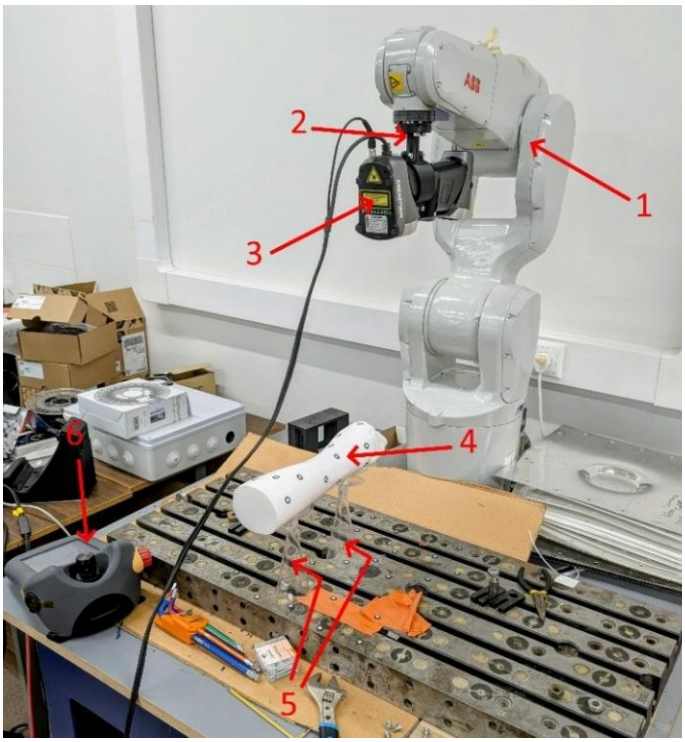

Fig. 18. Full Scanning Experimental Setup.
Here: 1 – ABB IRB 1200, 2 – adapter, 3 – HandyScan 700, 4 – 3D printed arm, 5 – see-through supports, 6 – control panel

Before any other tests can begin, the general scanner settings must be decided, most important of which is the laser exposure time, referred in the software as shutter time and measured in milliseconds. This setting determines how long the laser pattern is projected for, which can change results drastically. The general principle is that glossy or darker surfaces demand a longer exposure time, while brighter, matte surfaces allow the use of shorter exposure times. Usually, a higher exposure time improves results up to a certain point, when motion blur, artefacts and surface errors appear due to the scanner captured frames per second no longer being sufficient for keeping up with its own movement. Therefore, in essence, the exposure time limits how many frames per second can be captured, which in turn limits the theoretical maximum of points captured per second.

All scans in this work were done using VXelements software, which allows for many possibilities to modify scan results, although not much manual mesh modification is possible. Some of the settings that are important include: resolution, smart resolution, remove isolated patches, optimization mode, shutter. Resolution determines how many dense the cloud of captured points is, which is generally limited by exposure time, frames per second captured, scanner specifications (HandyScan 700 has an upper limit of 480,000 points per second). Smart resolution is essentially the application of algorithms that modify mesh density, for example making geometrically complicated areas more dense while lowering density in less important regions, in this project this feature was turned off, as it did not affect deviation values or surface area. Remove isolated patches is a great function that will remove floating artefacts or unintended capture of surrounding objects, in most cases this was set to 4 when finishing a scan. Optimization mode refers to finalization of each scan, where it is automatically repaired or enhanced, the one that affects mesh accuracy the least was chosen, called mesh enhancement. Shutter refers to laser exposure time discussed before, it can be set manually anywhere from 0.1 to 8 ms, the factory default is 0.6 ms. After each scan is done, the background is removed using clipping planes, an example of cleaning a scan is provided below (see Fig. 19).

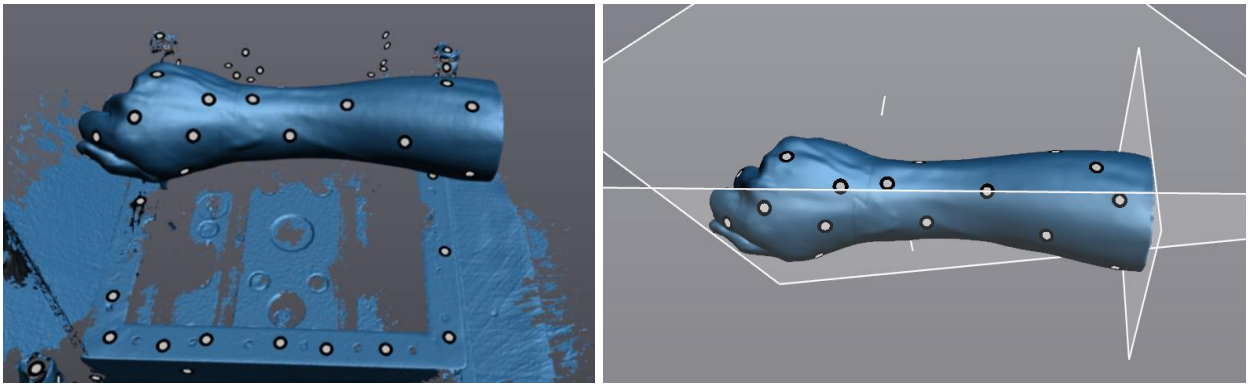

Fig. 19. Results of Scan Finishing Process in VXelements (left – before, right – after)

Throughout this work, experiments will mostly be assessed via scan surface area, after background and floating artefact removal, this is checked by navigating to properties of each scan. Although surface area is a reliable metric to assess scan results and in general, higher area means better scan, it does not tell the full picture of how accurate the scan in fact was. This is where root-mean-square error (RMSE) plays a key role, it is by far the most accepted metric of limb measurement, used in most of studies that analyse scan quality. Some research instead mentions standard deviation, but this is essentially the same thing, as the main difference lies where the distribution is centred. Standard deviation data distribution is centred on the mean $\bar{d}$, while RMSE is centred around zero (see Eq. 2, Eq. 3).

This project is no exception to this practice; standard deviation will be evaluated in tests where it is appropriate. The way that standard deviation is evaluated is through VXelements scanner software's integration called "VXinspect Quality Control", which allows to compare two meshes together. In most cases, the original STL mesh used for 3D printing is imported as the nominal reference, unless stated otherwise. The general workflow was as follows: import meshes, align the part to be evaluated to the reference, set up colour map, view calculation results. Parts were always aligned by using the built-in tool called surface best fit, which automatically finds the position with lowest deviation, an example is provided in Fig. 20. Relevant parameters for alignment are maximum distance, maximum

angle, number of iterations, throughout this work they were taken as 0.1 mm, 15° and 100 iterations, respectively. Colour map parameters are both visual and result affecting, the colour distribution and heatmap values used in this work were between bounds of -1.5 to 1.5 mm, with anything outside of the -0.15 to 0.15 mm window being considered error, this is a purely visual parameter that determines colour map intensity (Fig. 21). The ones that truly matter to the standard deviation results are automatic selection and calculation filter parameters. Maximum distance here sets how away points can be (if there are gaps or floating points), which was always used as 2 mm, maximum angle works in the same way but for angles – set to 90° in all tests, since the object is close to a cylinder and values beyond this did not affect the result. Surface maximum distance is the last parameter that matters, and it limits how far away (error wise) points can be to be evaluated, since models are all cleaned, this value does not change standard deviation so long as it is above the maximum error found.

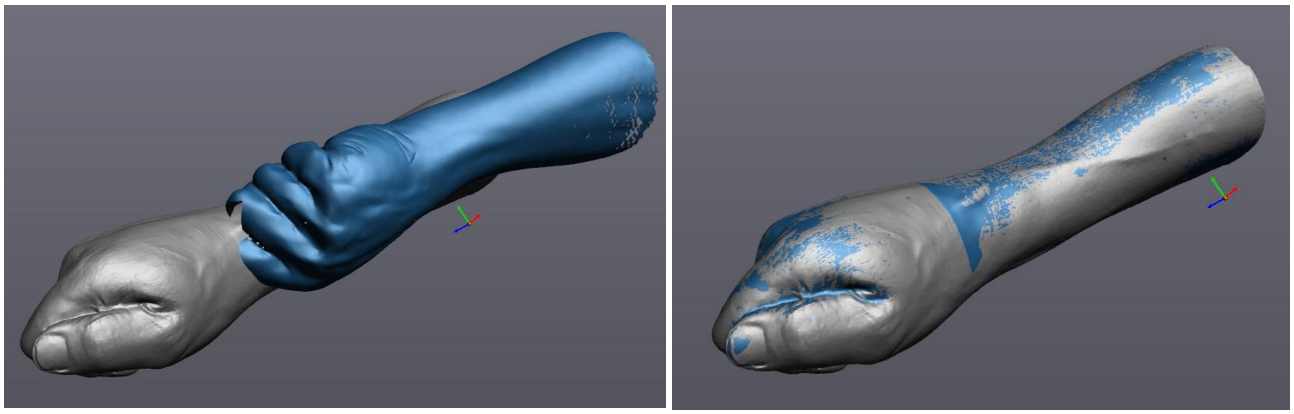

Fig. 20. Surface Best Fit Scan Alignment Showcase, Images Before and After

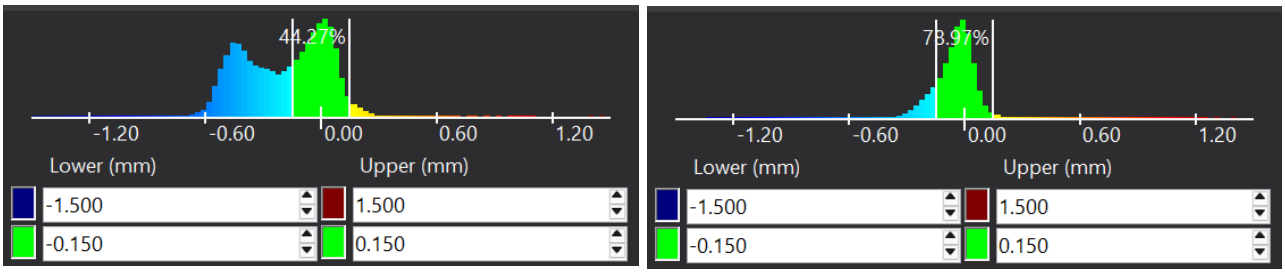

Fig. 21. Examples of Error Distribution Graphics in the Colour Map Setup.
Left – wide distribution, two peaks (bad result), Right – good result

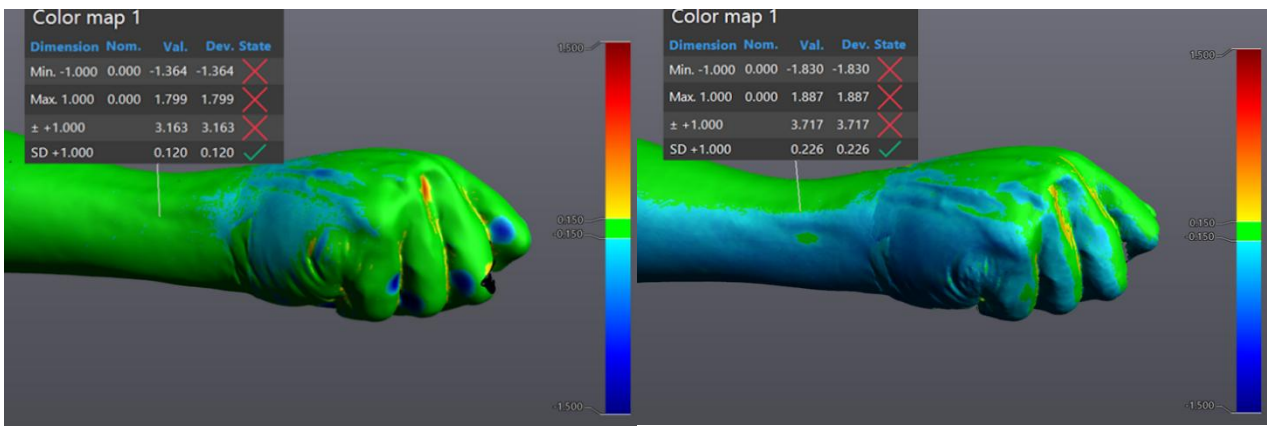

Fig. 22. Colour Map View with Main Results Displayed (red cross, green tick – not used here)

$$\sigma = \sqrt{\frac{1}{N}\sum\left(d_i - \bar{d}\right)^2}, \quad (2)$$

$$RMSE = \sqrt{\frac{1}{N}\sum d_i^2}, \quad (3)$$

where: σ is the standard deviation (mm); N is the total number of points; d_i is the signed distance of i^{th} point on the scan to reference surface (mm); $\bar{d}$ is the arithmetic mean of all d_i values (mm); RMSE is the root-mean-square error (mm).

3.1.3. Exposure Time Optimization

To find the correct exposure time and explore its influence on scan results, the same scan was repeated multiple times with varying exposure times, ranging from 0.5 ms to 5 ms, whereas the factory limits are 0.1 to 8 ms. Values above 5 ms were not included due to the appearance of artefacts and motion blur in the scans. A resolution of 0.8 mm was chosen to be used in these tests, which is high enough in density to show effects of other parameters, but not so precise that it could cause issues. The speed was chosen as 100 mm/s (max linear speed was the main speed factor), which should provide acceptable results for most exposure time settings. This also happens to be the factory safety limit set by the manufacturer for robot testing, any speed preset above v100 requires the use of auto mode and cannot be ran using the control panel. Each test scan was taken 3 times and the average result was used in drawing of plots, which can be found below (see Fig. 23, Fig. 24). In the first plot, surface area coverage is compared for different exposure times, looking at the result for white glossy material, it shows clearly that higher exposure times lead to higher surface area coverage, albeit with diminishing returns. In addition, anything below 1.5 ms yields poor results, as simply going from 0.5 ms to 1.5 ms resulted in 23 % more vertices. As a baseline, anything above 1.5 ms is suitable for the white glossy surface with the used speed, distance and resolution. Choosing higher movement speeds would require a lower exposure time, leaving 1.5 ms a safe choice for most configurations.

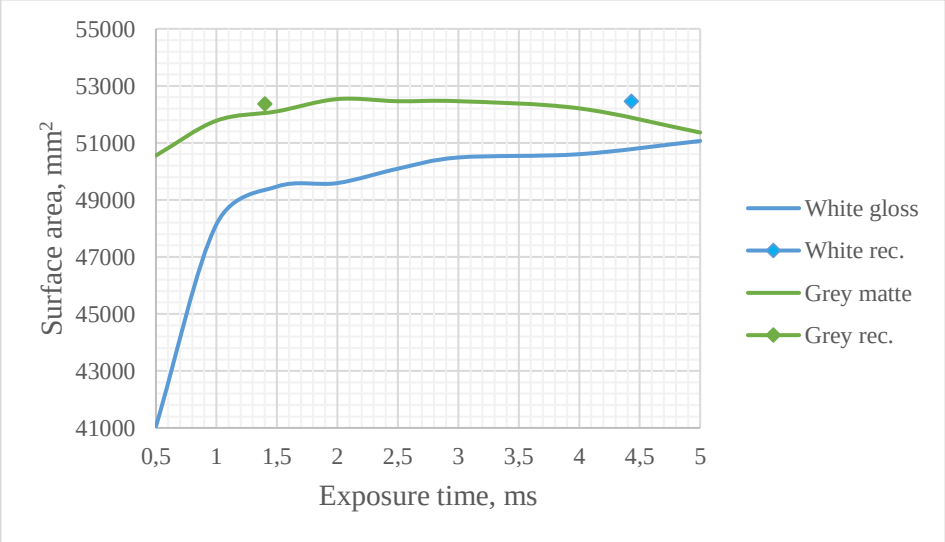

Fig. 23. Plot of measured surface area, mm^2 vs exposure time, ms for different materials. Settings used: 0.8 mm resolution, 100 mm/s speed, 335 mm distance to subject

Tests using the original white, glossy PLA surface of the hand replica would sometimes fail or have errors in them, which combined with highest area coverage appearing at very high exposure values

suggested that the surface finish is problematic. To solve this issue, the hand was sprayed with a thin layer of grey, matte priming spray. It is already known from the literature analysis that less reflective surfaces show better scanning results on average, but it was still important to confirm this. In the second plot (Fig. 24), surface standard deviation is compared at different exposure times. Surface standard deviation was retrieved from VXelements software, using the integration called quality control, where scans exported as STL meshes were compared to the baseline STL used for 3D printing the replica. As seen in the result plots, this small change in surface type changed results drastically, namely the surface area graph of the primed surface was much flatter, peaking at around 2 ms exposure time. In similar fashion, the standard deviation plot shows that surface quality of the scan diminished significantly for the white, glossy finish, which was much less of an issue for the grey, matte surface finish. To quantify this, on average, the matte finish had a 6 % larger average surface area recorded, with a 19 % higher minimum and 25 % lower average standard deviation, along with a 63 % lower maximum. The results reflect how the grey, matte surface finish is much more stable than a glossy, lighter surface.

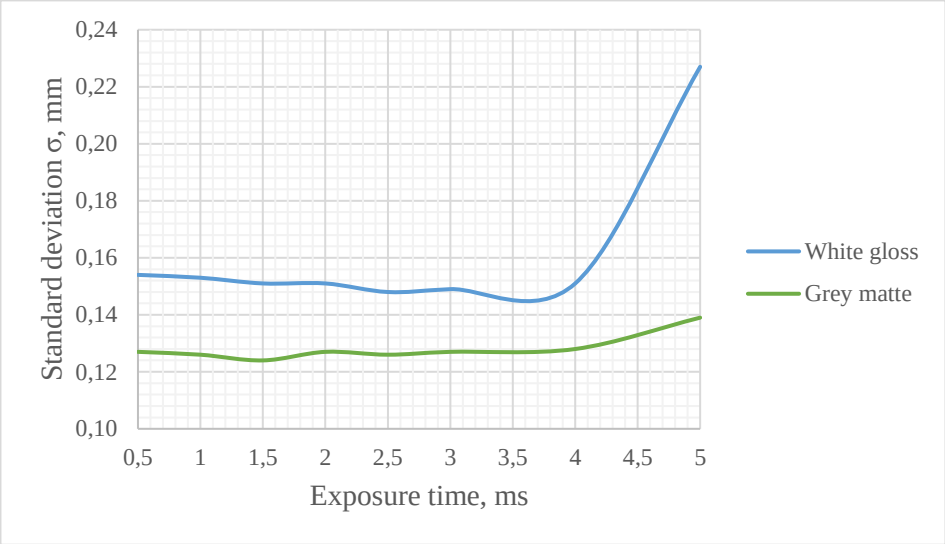

Fig. 24. Plot of standard deviation, mm vs exposure time, ms for different materials. Settings used: 0.8 mm resolution, 100 mm/s speed, 335 mm distance to subject

As it turns out, the software that was being used for this already had an option to optimise scanning parameters, which requires a sample scan that is done real-time. This is especially useful in this use case, since the path followed by the robot is always the same, at a constant velocity. Therefore, theoretically, this function is utilized perfectly in such a case, which indeed was the case, with the exact same result (4.43 ms) being presented 3 times out of 6 for the white, glossy finish. Using this setting, some of the highest vertex counts were recorded and it was chosen as the one to use in further tests with the white material, unless issues due to movement speed arise, in which case the same feature can be used to determine a new exposure time. For the grey, matte surface this was not as useful, as the program suggested exposure of 1.39 ms, which was close to the best performing 2 ms, but not as good. Average results with the recommended exposure times for both finishes are included in the surface area graph (Fig. 23) as diamond shaped points called “White rec.” and “Grey rec.”, also this feature allowed to confirm that the distance to subject was chosen correctly, with the distance meter always staying in the perfect range (green). This configuration process is shown in the figure below (Fig. 25), there in the centre is the full laser pattern with a visualization of what the camera

currently sees, yellow colour indicates that the exposure is ideal. The bar on the left of the figure is a distance indicator that changes colour to light blue when the scanner is too far away from the object and turns red when it is too close. On the right of the figure is where the automatically adjusted shutter speed (laser exposure time) is displayed.

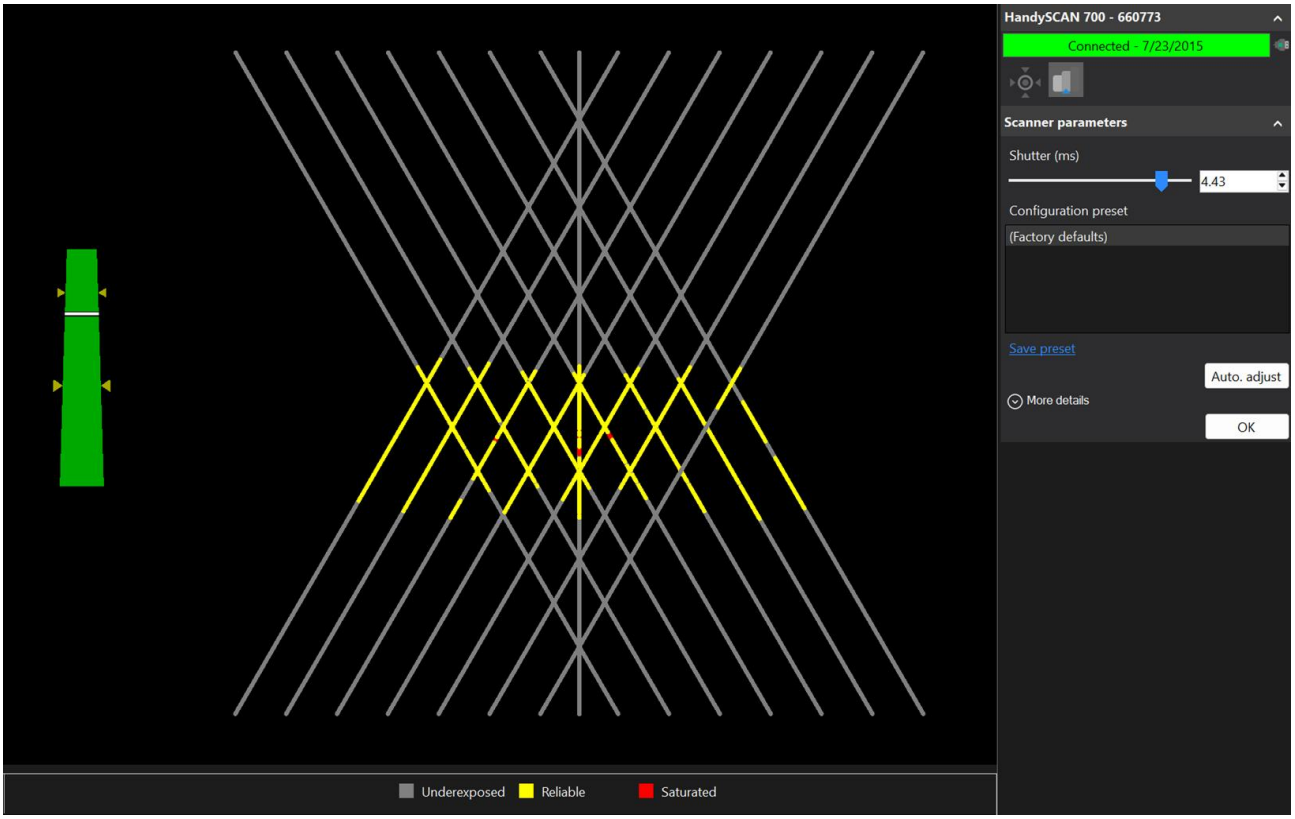

Fig. 25. Scanner Configuration Window

3.1.4. Testing of Deviation Caused by Fused Filament Fabrication

After the exposure times were decided on (glossy – 4.43 ms, matte – 2 ms), the following step was to check for repeatability and reproducibility of scans. To find out these metrics, 7 tests were conducted with each surface finish, using the same settings for all of them, comparing these to each other allowed to test how much variability there was. The settings used were a resolution of 0.8 mm, toolhead movement speed of 100 mm/s, 335 mm distance from scanner to object and a total distance of 240 mm covered in the X axis. In this case, scan stitching was also done, since future tests will be doing the same, it is logical to include this part of the scanning process, although it could slightly obscure the scanner noise. Scan stitching is done in the scanning integration of VXelements, by importing scans of both sides of the hand, creating points on 3 targets that are matching between both scans and then aligning one of the scans to the other by using the entity-based alignment feature and selecting the same points on both scans. After alignment, the merge scan feature is used, which automatically combines both scans into one, removing any irregularities along the way. Normally, this is a difficult process, but since targets are used and the replica arm is not moving, it becomes relatively fast and simple, taking 1-2 minutes to complete. All major steps are visualised in Fig. 26, where the first part shows scans that are just imported, which are usually aligned randomly. The second part shows the creation of points directly on targets, which are then used to align the two scans. Third part shows scans after alignment in the merging step, with also some scan parameters visible, in this case

resolution was 0.6 mm, smart resolution (post processing algorithm) was off and remove isolated patches (areas largely disconnected from the rest) was set to 3.

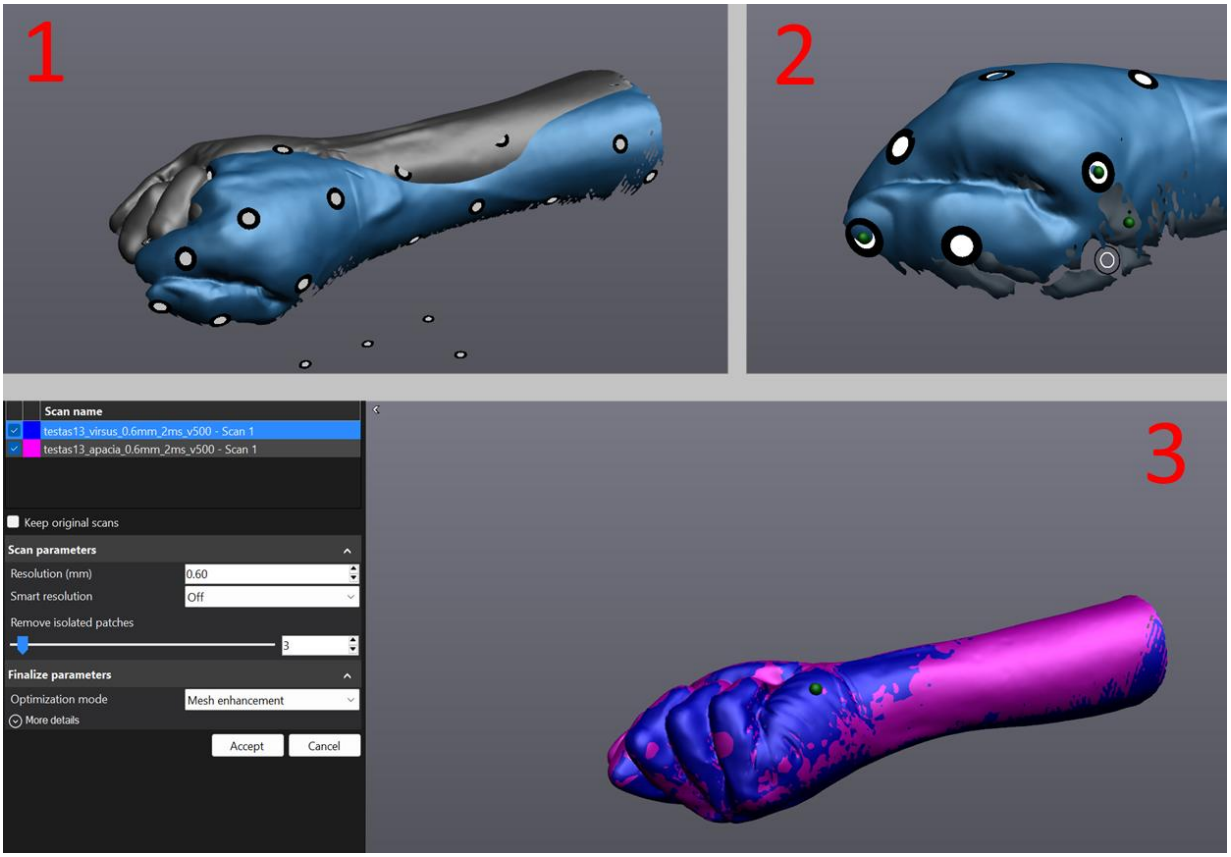

Fig. 26. Scan Stitching Workflow in VXelements.
Where 1 – scan importing, 2 – point creation (green dots), 3 – mesh merging

There is bound to be a significant difference between the original STL and scans of the 3D printed replica, since FFF cannot perfectly replicate a mesh of such complexity as the human arm. In addition, the full arm could not fit in a printing bed, so it had to be done in two pieces, creating more inaccuracy in the connection area. A reliable way to quantify this difference is to take some scans of the arm and then compare each of them to the original STL, all scans should contain more or less the same amount of error which will correspond to print error, along with some variance. Finding this variance is another goal of these tests, this can be done by first taking 7 scans and comparing 6 of them to the first one. The standard deviation found from this should be almost entirely from scanner noise, which will show repeatability, it can also then be quadratically subtracted from the deviation when comparing to the original STL to isolate only the printing error. Scans of both the top and bottom of the arm were done for both the grey matte and the white glossy surfaces, resulting in 14 scans after merging, the test results are listed in the table below (see Table 5).

In the result table are provided the total standard deviation, which was retrieved from comparing to the original STL, corrected standard deviation is the measured print error, retrieved by quadratically subtracting the scanner noise from the total. Something to note is the fact that print error is different for the glossy and matte surfaces, this difference either appeared due to more material being on the arm after spraying, or due to not all of scan error being subtracted. Most notable is the scanner noise found, for the white glossy surface this was an average of 0.0560 mm between scans, for the grey

matte surface it was an average of 0.0277 mm, an improvement of 50 %. In contrast, difference between total standard deviation of the two surfaces was only 21 %, this is another example of how big an impact a different surface finish can have. The percentage of hand surface area covered is another metric that was tracked by comparing to the surface area of the original STL, but there was no difference between the two surface finishes.

Table 5. Summary of Repeatability Test Results

Scan no.	White glossy			Grey matte		
	Total std. dev., mm	Corrected std. dev., mm	% of area covered	Total std. dev., mm	Corrected std. dev., mm	% of area covered
1	0.156	0.146	97.44	0.136	0.133	97.44
2	0.174	0.165	97.15	0.128	0.125	97.15
3	0.170	0.161	97.21	0.133	0.130	97.21
4	0.169	0.159	97.12	0.134	0.131	97.21
5	0.163	0.153	97.29	0.134	0.131	97.47
6	0.170	0.161	97.19	0.132	0.129	96.74
7	0.172	0.163	97.22	0.133	0.130	97.36
Average	0.168	0.158	97.23	0.133	0.130	97.25

Overall, the robot of choice, ABB IRB 1200, mounted with the HandyScan 700 scanner achieved a high level of repeatability, with surface area varying by less than 1 % and a scanner noise that was significantly less than the manufacturing error representing 66.6 % and 79.2 % for the white and grey surfaces, respectively. This result was expected, since 3D printing is known to struggle to replicate round objects, due to limiting factors such as extrusion layer height, nozzle diameter, supports and fill pattern. Corrected standard deviation stands for deviation with scanner noise accounted for, which is subtracted quadratically to avoid ambiguity in tests where standard deviation is already very low. In some future tests, it would be more valuable to compare results by using the best overall scan as reference, rather than the original hand before 3D printing, since that would isolate any deviations to be not related to manufacturing.

3.1.5. Evaluation of Toolhead Movement Speed's Effect on Scan Results

The next parameter to be evaluated is robot toolhead movement speed, which could be considered the main aim of this work, as it has to do with how fast a scan can be done without sacrificing accuracy. As mentioned before, toolhead speed is set to one of the available presets in the robot code, tested and prepared by the manufacturer. The ones chosen for testing are provided in the table below (see Table 6), with values taken from the official ABB RAPID programming language documentation [26]. Presets are used since manually changing each speed would increase project scope far beyond what is currently possible for the timeline, also since these are created and rigorously tested by the manufacturer, there is virtually no risk of the robot malfunctioning. Since in each of these presets, the maximum rotary speeds are defined at much higher relative values to the linear speeds, total scan time is mostly influenced by linear speed limit, with orientational speed only playing a role in the highest of settings used. The total scan time with each of these speeds is presented in a figure below (see Fig. 27), an important note is that increasing speed past 1000 mm/s had strongly diminishing effects on scan time due to the nature of the path the robot has to follow. Since the path requires the

robot to rotate constantly, linear speed reaches a cap at a certain point, where it becomes limited by the maximum angular speeds for robot link orientation.

Table 6. Predefined Speed Data Presets Used in the Code and Tests [26]

Preset	Toolhead Speed, mm/s	Orientation Speed, °/s	Linear ext. axis, mm/s	Rotating ext. axis, °/s
v100	100	500	5000	1000
v300	300	500	5000	1000
v500	500	500	5000	1000
v800	800	500	5000	1000
v1000	1000	500	5000	1000
v1500	1500	500	5000	1000
v3000	3000	500	5000	1000

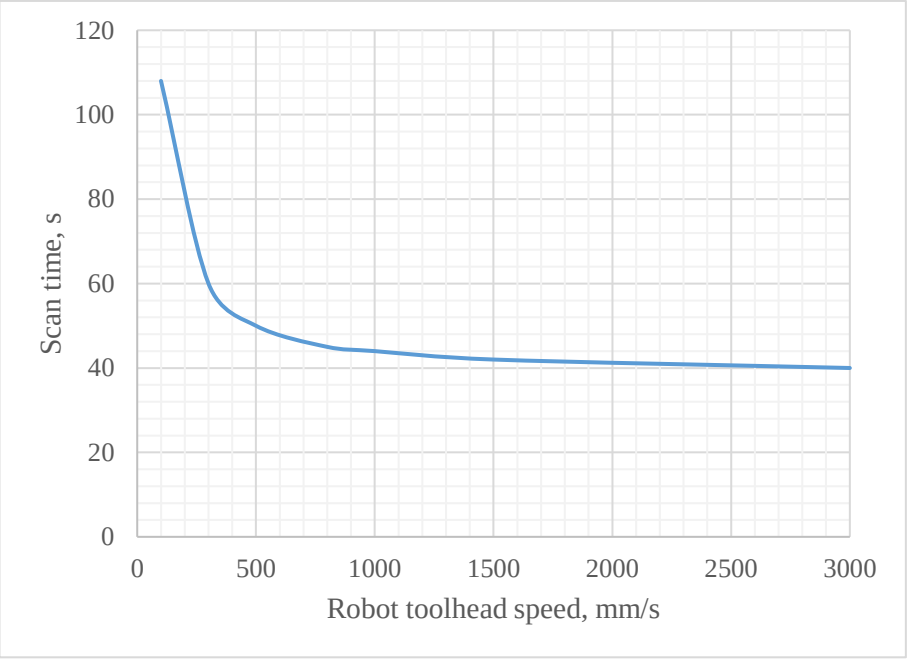

Fig. 27. Graph of Toolhead Movement Speed, mm/s vs Total Scanning Time, s

From this test onwards, only the grey matte surface finish was assessed, since its effects on scan results were already demonstrated and it was much more stable with better meshes. The main scan quality metrics that were measured once again was recorded surface area, mm^2 and total standard deviation, mm. Surface area shows how close to point cloud saturation the scanner gets, in other words, how much of the total data is captured. Standard deviation is the best measure of scan accuracy that there can be for human limb measurement, as it shows how close to the reference mesh the captured surface is. In general, the larger the deviation, the wider the data distribution bell curve becomes, lowering the certainty of each point's location, the lower the deviation – the better.

Four varying resolutions were chosen to be tested, to visualise how fast the scanner can move for each resolution, in addition to the toolhead speeds, namely – 0.2, 0.6, 1, 2 mm. The expectation is that lower resolutions will start failing at lower movement speeds than higher resolutions, since the

main limiter is how many points the scanner can capture per second. The scan meshes were compared after stitching, with each scan being repeated 3 times and the average values being used for result plotting. Each scan used an exposure time of 2 ms, distances are the same as before – 335 mm object to scanner distance, 240 mm forward distance travelled in the X axis. Toolhead speeds beyond 500 mm/s caused the 0.2 mm resolution tests were not able to capture almost any surface area, so they are not included in the results. This effect got progressively worse as speeds were increased further, this progression is visualised below (Fig. 28, Fig. 29).

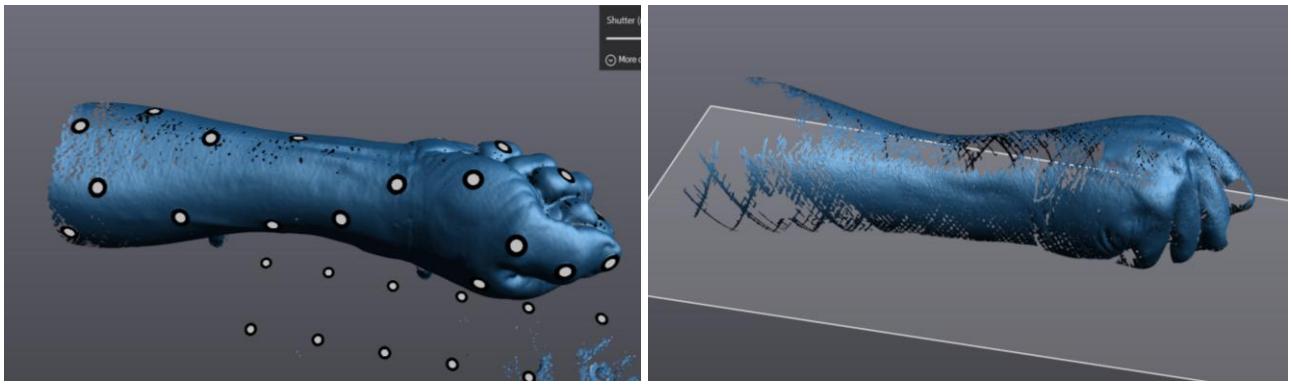

Fig. 28. Maximum Resolution Scans (0.2 mm), Left – 300 mm/s, Right – 500 mm/s

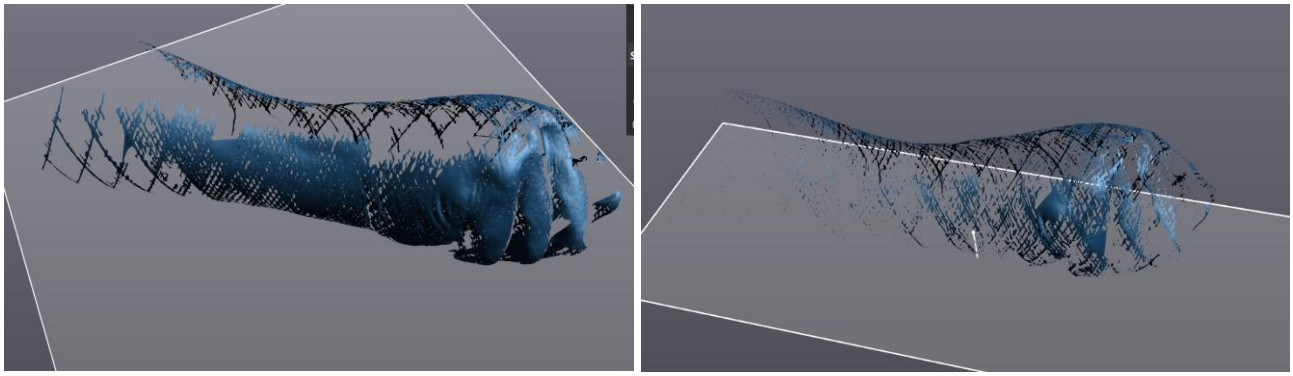

Fig. 29. Maximum Resolution Scans (0.2 mm), Left – 800 mm/s, Right – 1000 mm/s

As illustrated in the graph of speed vs covered surface area (Fig. 30), all of the tested resolutions had the largest surface area meshes at 100 mm/s speed, which would indicate that the best results should be at this speed. This was proven not true however, standard deviation data indicates that instead, a speed of 500 mm/s was optimal for all resolutions except 0.2 mm, this is also visible in the plot (Fig. 31) and 2 mm, which in fact excelled at even higher speeds. These results show a clear trend, the higher the resolution, the more surface area can be captured in a sweep and the lower the standard deviation of the mesh retrieved. Regarding the tests with 0.2 mm resolution, while at a slow enough speed, it was by far the most accurate, but much more prone to scanning issues and unusable at higher speeds as there was not enough surface area to work with. To visualise the trend better, a trendline was generated using a 3rd order polynomial to predict the next 500 mm/s of speed. It is still difficult to conclude which configuration is best however, as clinically acceptable accuracy of 1 mm is achieved in all cases, but this is only applicable to prosthetic's sockets and similar use cases. For the purpose of this project, the overall best combinations will be considered, which in this case was a speed of 500-800 mm/s used with 2 ms laser exposure time and 0.6-1.0 mm point cloud resolution.

Under these conditions, faster speeds are clearly preferable, since in most cases there is an ideal speed for bests quality results, as seen in the standard deviation graphic.

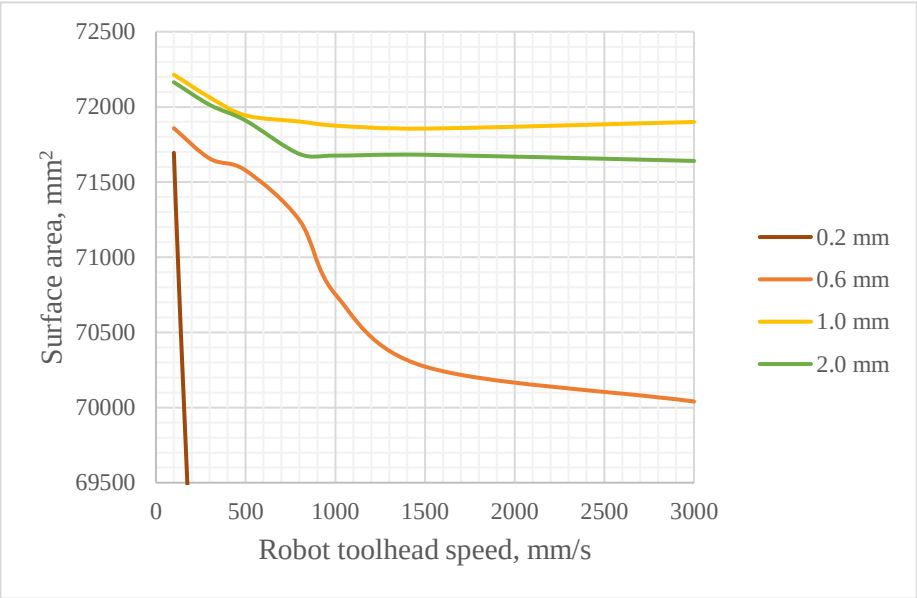

Fig. 30. Plot of Toolhead Movement Speed, mm/s vs Surface Area Covered, mm^2 at 4 Resolutions (0.2, 0.6, 1, 2 mm)

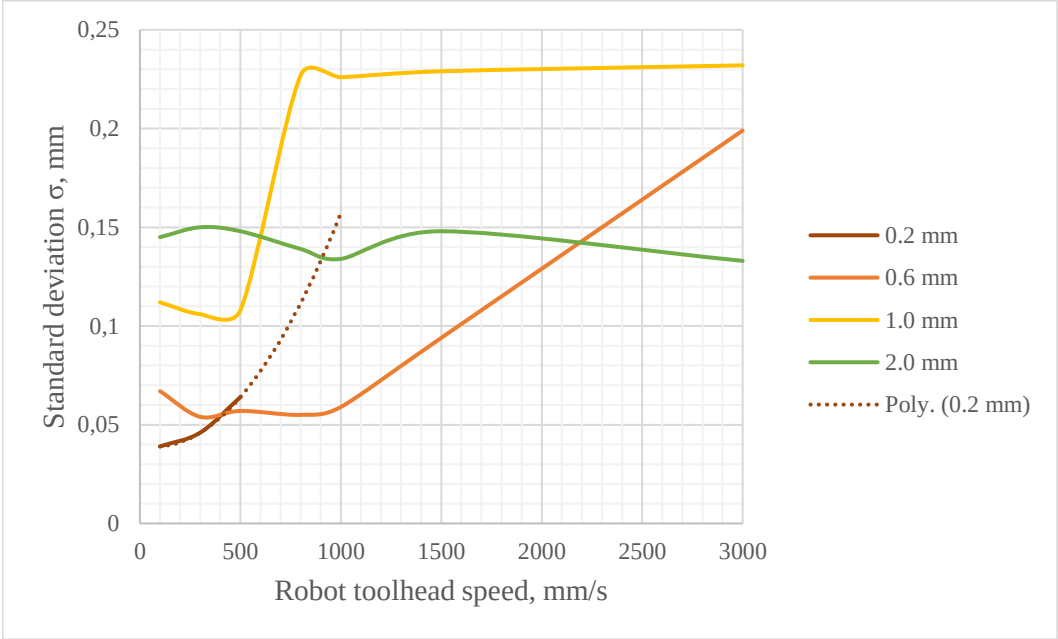

Fig. 31. Plot of Toolhead Movement Speed, mm/s vs Standard Deviation of the Surface, mm at 4 Resolutions (0.2, 0.6, 1, 2 mm)

Although standard deviation is the most reliable metric for scan evaluation, deviation extremes in the form of maximum and minimum error can also be insightful. In some fields of medical measurement, clinically acceptable accuracy is cited as anything below 1 mm error [8, 15]. This experiment's highest deviation values are listed in the table below (Table 7), where a general trend of higher resolution – error extremes closer to zero can be observed. If abiding by the maximum/minimum error having to be closer to zero than 1 mm rule, only the 0.2 mm and 0.6 mm resolution tests at 100

mm/s would be acceptable. This metric does not appear as reliable numerically however, since values seemingly fluctuate at random and resolution does not affect it as significantly as standard deviation or surface area coverage did.

Table 7. Average Minimum and Maximum Error in Tested Scanning Configurations

Speed Preset. mm/s	**0.2 mm**		**0.6 mm**		**1.0 mm**		**2.0 mm**	
	Min. error, mm	**Max. error, mm**	**Min. error, mm**	**Max. error, mm**	**Min. error, mm**	**Max. error, mm**	**Min. error, mm**	**Max. error, mm**
v100	-0.684	0.889	-0.653	0.938	-1.642	0.914	-1.660	1.804
v300	-0.667	1.645	-1.141	0.412	-1.417	0.755	-1.724	1.951
v500	-1.308	1.774	-1.337	0.739	-1.596	1.506	-1.816	1.949
v800	-	-	-1.159	1.689	-1.475	1.429	-1.909	1.956
v1000	-	-	-1.198	1.695	-1.675	1.707	-1.530	1.961
v1500	-	-	-1.205	1.656	-1.617	1.521	-1.933	1.860
v3000	-	-	-1.258	0.902	-1.482	1.528	-1.447	1.995

3.1.6. Influence of Scanner Operator's Experience on Results

Now that the optimal settings ranges have been decided on, the following step is to quantify the exact benefits of automating the scanning process. To assess this, two scanner operators of different skill levels (amateur and expert) were given the task to scan the hand replica and compare their results to the robot automated setup. The operators were given one test scan and then scanned the top and bottom of the hand three times each, three scans were also done with the robot arm for reference. Settings used in these were a resolution of 1.0 mm, 2 ms laser exposure time, robot settings included v500 preset, 335 mm distance to subject. Main metrics of evaluation are total scan time (top and bottom combined), excluding scan stitching time, surface area covered in one scan (top only) and total standard deviation of the surface. Results are presented in bar charts below, values used are averages between the three scans (Fig. 32, Fig. 33, Fig. 34).

To summarize, the amateur operator covered the least surface area, likely due to inexperience with the software computer interface and not being familiar with best scanning practices. Since they did not focus on covering as much of the area as possible, the scan took less time than that of the expert, 127 seconds on average. The more experienced operator took longer in each scan, moving the scanner more slowly and carefully, with a focus on covering as much of the surface as possible, which resulted in longer scan times, 205 seconds on average. Robot arm was able to achieve much faster scan times at 45 seconds on average, which was already recorded in previous tests. Surface area was measured in mm^2 from which the percentage of area was calculated using the original hand mesh's area. The expert operator achieved an average of 83.1 % surface area covered, while the amateur only had 67.8 % and the automated one had 76.2 %. Higher area values are desirable despite using scan stitching, as more area overlap between the top and bottom scans will reduce the error margin, as shown in previous tests. Standard deviations between the three did not have any significant difference, varying by no more than 2 %, which shows that the automated solution does not lose out on accuracy, despite scanning multiple times faster. The robot arm had higher maximum errors however, at around 10 %

larger values than the expert and amateur scans. Worth noting that the amateur operator also had one failed scan, which was allowed to be repeated.

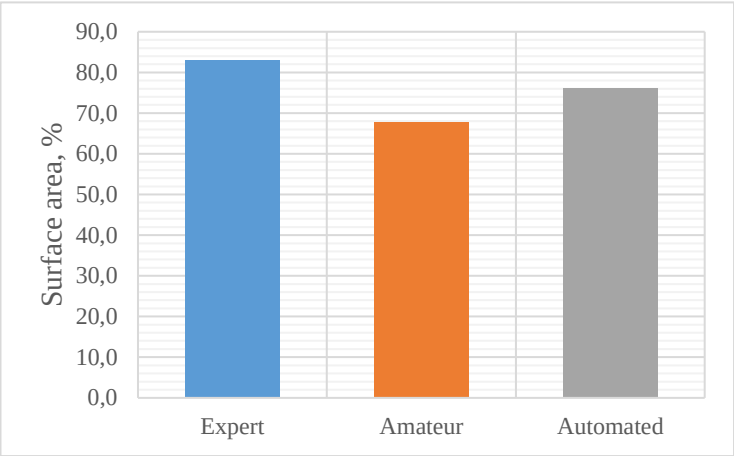

Fig. 32. Bar Chart of Average Surface Area Covered in Top Scan, %

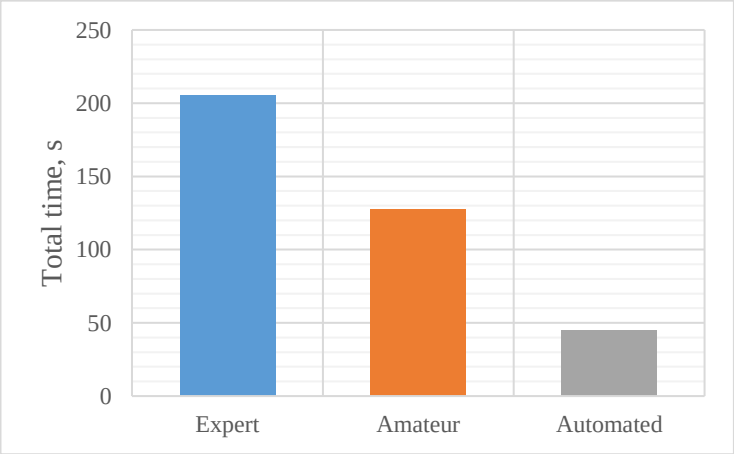

Fig. 33. Bar Chart of Total Scanning Time, s

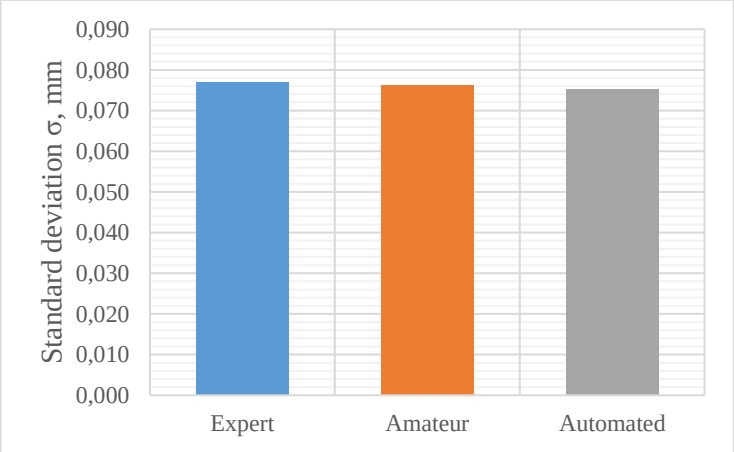

Fig. 34. Bar Chart of Standard Deviation, mm

This test shows that the robot arm can keep up in performance with an experienced user for a static arm scanning test, which means that the gain in scan speed comes at virtually no cost in result quality.

The significantly shorter scanning time will improve results far more when scanning a real hand, since the longer the scan time, the higher the odds for involuntary movement or angle change at joints, as discussed previously. Future tests could seek to reduce the scan time further, since angular speeds were not changed in this work, it could be a way to go down below 10 seconds per scan, compared to the current minimum of 22.5 seconds. Also, some tests could be done at higher resolutions, which benefit greatly from faster movement speed, as shown in the previous experiment, this would likely swing results more in favour of automation since people cannot scan as fast.

3.1.7. Qualitative Assessment of a Person's 3D Scanned Hand, Real World Test

As a final trial for the automated system, a real person's hand was scanned using the found optimal parameters of 800 mm/s (v800 preset) robot arm movement speed, 0.6 mm scanner resolution, 2 ms laser exposure time and 335 mm scanner-subject distance. A higher speed configuration was preferred to minimise the odds of joint angle change or hand movement in between or during scans. Markers were once again applied all around the arm's surface, in similar fashion as the static replica, albeit only 15 of them, more than two times less. Some issues were still apparent during the whole process, as a satisfactory result was only achieved on the 4th attempt and required extra post-processing compared to the static replica arm. Surface area problems appeared (Fig. 35) due to slight involuntary movements during scanning, which caused motion blur, as well as reflectivity, since the real hand surface was not primed with any spray. This could be solved with relative ease through the use of sleeves with pre-applied markers, or the use of more recently developed scanners which outperform the used scanner in every way. Despite surface issues, all failed attempts did so due to joint angle change that prohibited merging of scans, as it was impossible to align them (see Fig. 36).

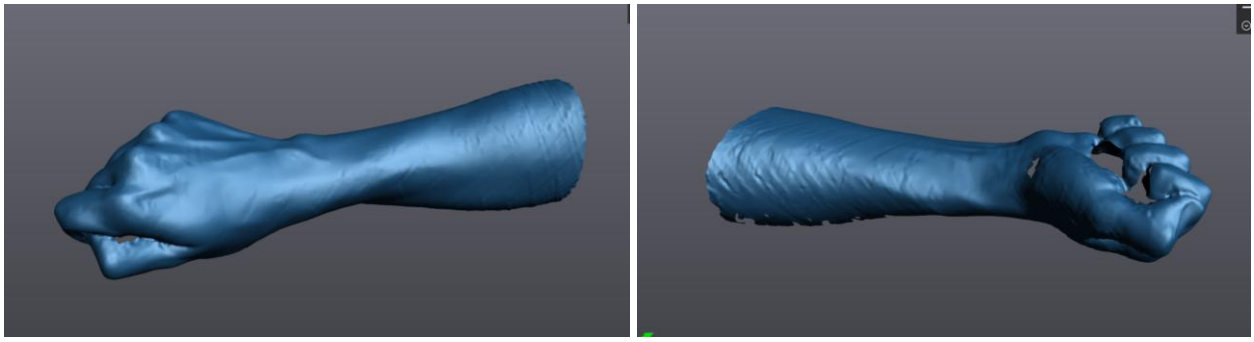

Fig. 35. Automated Real Hand Scans with Poor Surface Finish (motion blur), Top and Bottom Examples

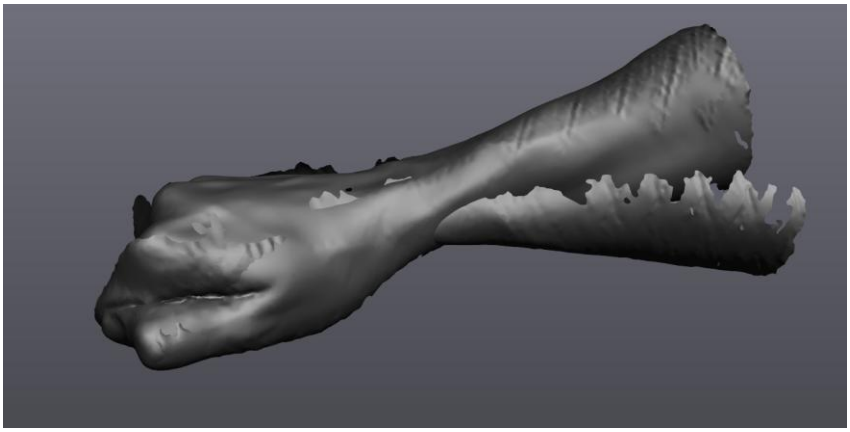

Fig. 36. Failed Stitching Due to Joint Angle Change Example

The scan that was successfully completed still required some post-processing, which tampered with quantifiable results, originally, the model had 170,165 vertices, a surface area of 66,134 mm^2 and a volume of 800,464 mm^3. After it was fixed, these went down to 77,903 vertices, which is to be expected since a rough surface was smoothened, 60,285 mm^2 area and 776,846 mm^3 volume. Change in area was much larger than the change in volume, which is not a surprise since the area was fingers that were removed from the mesh. This measured volume shows that the second person's hand is 33 % lesser in volume than the first one and in turn – smaller.

For any future tests, better quality supports must be developed and used, as motion blur caused by movement during scanning will undoubtedly have a profound, negative effect on standard deviation of these scans. Aside from better supports, robot arm speed could be increased further, although it was shown that this is a strong limiter of usable resolutions. It might be a requirement to use a newer, more capable scanner to go to faster speed settings, especially if radial speed is also modified. Furthermore, it would be significantly more effective to use a robot arm that can go 360 degrees around the arm, avoiding scan stitching altogether, since this would reduce the negative impact of angle changes, which seemed to happen mostly when flipping the arm over to the other side. Utilizing specialised sleeves to cover the arm before scanning is recommended, since human skin can be highly reflective, or very dark in some cases, which means more of the laser is absorbed. A lot of these factors are less impactful on newer scanners that use other methods of capture, than red laser patterns or combine laser with some form of photogrammetry systems.

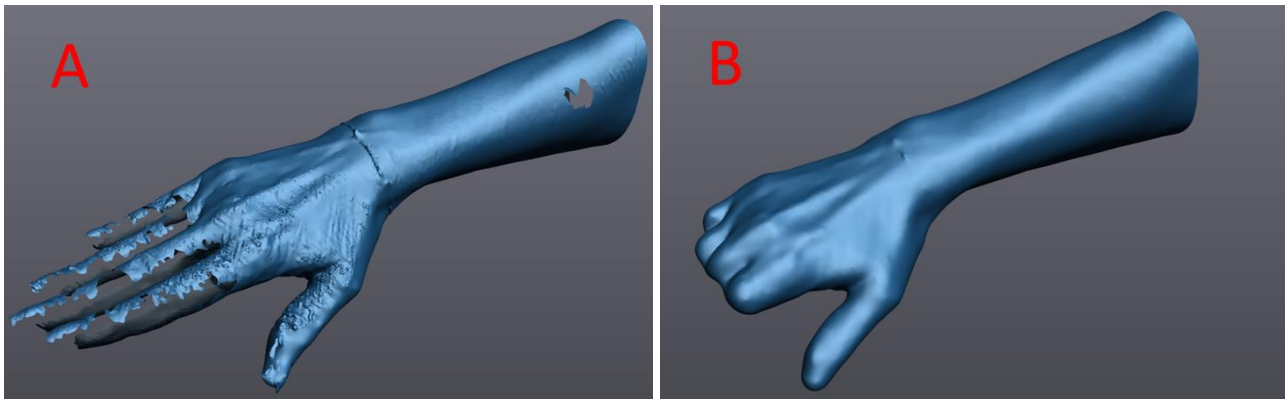

Fig. 37. Successfully Automated Real Hand Scan, Before Post-Processing (A) and After (B)

3.2. Discussion and Result Contextualisation

Finally, the results of this chapter must be compared to that of other authors of similar works in order to contextualise and summarise the findings. Initially, the effect of surface reflectivity was tested, with the grey matte primer spray increasing accuracy to an average of 125,627 vertices and SD (standard deviation) of 0.127 mm from the 119,773 and SD of 0.151 mm measured for the glossy white. This was equivalent to a 5 % increase in point count and 16 % reduction of scanner noise. Other studies that were analysed did not focus on the negative aspect of skin reflectivity, as far as it seemed, only one study mentioned skin preparation and that only included marking key points with a Devon skin marker [16]. Nevertheless, comparing to that study, this work achieved roughly 40 % lower standard deviation values against their average of 0.25 mm SD. Although not perfectly comparable since a real person was being scanned in the mentioned study, it can be comparable since the face was being scanned, which is much more static than limbs when supported.

Afterwards, scanner noise was measured to be around 0.0277 mm for the grey matte surface, an increase of roughly 50 % from the initial white glossy surface. It is estimated that such low noise is possible due to the stable nature of movement, allowed by the use of automation via robot arm. Also, this noise was about 5 times less than the rest of the SD, which indicates that a much larger part of the deviation comes from accuracy of the FFF process or automation parameters and not scanner noise. The results retrieved in this case are very high-precision, comparing to another study that mentioned measured scanner noise [17], it was reported that their tests on a phantom hand yielded an average of 0.11 mm noise, which is 75 % larger. In the best-case scenario of 0.2 mm resolution at 100 mm/s, an average of 0.039 mm SD was achieved, on par with another study that achieved 0.05 mm average SD [8]. This means that 20 % lower SD was measured, despite the other study using a more modern Artec Spider scanner, though worst case point error was worse, possibly due to scan stitching.

On average, surface area covered in a scan only fell 2.2 % on average when increasing speed, with the exception of the 0.2 mm resolution tests. This is significantly lower than another study that attempted to decrease scan time by accelerating scanning to finish under 30 seconds, where the authors noticed a loss of roughly 15 % foot surface area [20]. An example of the advantages that a constant, error-free path provides, whereas a human operator inevitably fails when accelerating. Although surface area and quality was lost in the mentioned foot scanning study, they did manage to complete a single pass scan in 26 seconds, which is admittedly close to the robot's achieved 22 second scan of one side. In terms of total time spent to retrieve a full scan, the automated robot setup allows for model to be ready in 2-3 minutes, which is comparable to another study that listed a full leg scan taking approximately 3 minutes [18].

Regarding acceptable error criteria, it is sometimes mentioned that -1 to 1 mm is a band of error that is suitable for clinical use, which in this work only 0.2 mm and 0.6 mm resolutions at 100 mm/s speed (v100 preset) satisfied such a condition. This does not however seem to be a universally true metric for accuracy, since another study accepted up to 1.8 mm max error in models when SD was below 0.2 mm [19]. Assuming a similar maximum, v300-v500 preset range would now be acceptable, which is a much more realistic result. Also, this setup consistently outperformed a photogrammetry rig that had similar area coverage and scan time, but resulted in 0.6 mm SD [10], a value much higher. Finally, an obvious advantage over some of the manual scanning studies is that the process is semi-automated in this project. With a robot arm that has larger maximum rotation angles, enabling 360-degree scanning, the process would no longer need stitching, allowing for full automation. In such a case, only a technician would be needed for scanning, rather than a professional doing active labour.

Table 8. Summary of Result Comparison to Other Studies

Study (ref.)	Limb, Scan Method	Average SD, mm	Max deviation, mm	Avg. Scan Time, s
This work	Hand. IRB 1200, HandyScan 700, 0.2 mm res., 100 mm/s	0.039	± 0.89	108
[8]	Hand. Artec Spider	0.05	± 0.6	-
[10]				
[17]	Hand. Structured light vs CT	0.3	± 0.84	90-180
[19]	Below knee loss limb. Structure Sensor (ToF)	0.18	± 1.8	180
[20]	Leg. Structure Sensor (ToF)	0.4	± 2.4	26

Study (ref.)	Limb, Scan Method	Average SD, mm	Max deviation, mm	Avg. Scan Time, s
[13]	Hand. 50 camera photogrammetry	0.6	± 1.2	90

As a small note, there was an initial attempt to connect this work to plastic sheet forming of prosthetic sockets, which has potential to outperform 3D printing for complex, multi-radial surfaces with multiple peeks. The robot code that was developed in this project can very easily be modified to be used for instructing the robot arm to form complex surfaces like the types mentioned, while the experimental setup would not have to be changed much (example in Fig. 38). Such an application of the robot arm would combine perfectly with the automated scanning setup, although an algorithm that could replicate these surfaces from 3D scans in commands would be need to completely connect the two. Another challenge is the surface heating, which would have to be applied locally in order to allow the plastic to bend without breaking, example prototypes that this could look like are provided below (Fig. 39). Such a solution highlights the potential future prospects that could follow this project, leading to reduced waste of similar product manufacturing. This kind of thematic is a very relevant engineering direction, especially with European projects like Horizon Europe that have funding of billions of euros for supporting environmentally friendly, innovative projects like this, especially so since it also relates to the medical field.

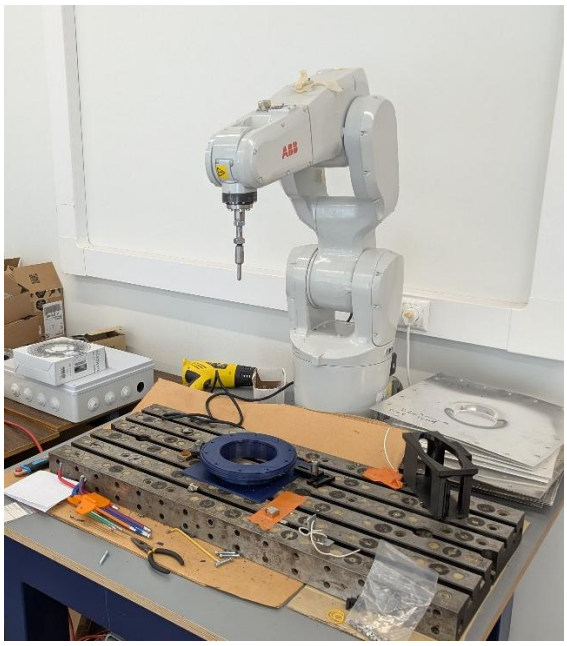

Fig. 38. Sheet Forming Setup

Fig. 39. Example Formed Knee Surface Part.
Where left image – outside, right – inside

To explain again the areas that need follow up research to focus on, sheet forming is a great example of a relative direction that this could go. Combining 3D scanning, printing and sheet forming into one workflow should have great benefits for prosthesis manufacturing. To explore this area, further research should be conducted into 3D printed part forming via robot arm under differing heating conditions, toolhead type and orientation. Apart from this, the areas highlighted before should be focused on, namely hand support development and testing with other hardware. Another promising prospect could be to dive deeper into the deep-learning algorithms being developed recently, such as CAPE (clothed auto person encoding) [29] that can do mesh fitting onto human body shapes or PoseNormNet [30], a model capable of normalizing the position of a human mesh. Similar algorithms could be adapted to use with human limbs, allowing for more robust error correction.

3.3. Chapter Summary

To briefly describe this chapter, the scanner HandyScan 700 (2015 ed.) attached to the robot arm IRB 1200 and were successfully used to prepare a workflow where one side of a hand can be scanned in as fast as 21 seconds with a 2 minute time to fully complete mesh, including scan stitching. Two different surface finishes were tested, with a grey matte primer decreasing SD from 0.151 to 0.127 mm for those tests, in addition, system noise of 0.0277 mm was found. Best compromise between speed and quality was for scans of 0.6-1 mm resolution and 300-800 mm/s robot toolhead speed. The highest quality scans were at 100 mm/s with an average SD of 0.039 mm, while faster speeds stayed at around 0.1 mm SD. Scan accuracy turned out to be scanner and resolution limited, rather than path related, since a novice user, expert user and robot all achieved nearly identical SD values (0.76, 0.77, 0.75 mm respectively) over multiple scans. The system still had issues with scanning a real hand, indicating the need to improve the support system, utilise a custom-made sleeve or swap to a 360° capable robot arm. Tests stood up to other author's works, outperforming (SD lower by 20-40 %) at the slowest speed of 100 mm/s, or matching quality in the 300-800 mm/s range, doing so while retaining a very high repeatability due to being automated. Best practices found in this work not only quantify the automated system's performance but can also be applied to manual scanning.

4. Potential Economic and Environmental Benefits

4.1. Setup Cost and Savings per Year Estimation

Economically, there is great potential for automated human limb scanning, as such an adaptation can save significant amounts of time. On its own, the system used in this work is at least 3 times faster than the average human operator, not to mention the possibility of eliminating human work almost entirely. Since this kind of technology has many different applications spanning multiple industries, to fully analyse its economic and environmental impact would require a project of larger scope. To fit within the initial plan of this work, the main focus will be just one example, improvement of plaster casting prosthetic sockets by automating measurements using the described 3D scanning setup and sheet-forming or 3D printing them. This is relevant due to the large waste of time and materials that this process typically entails, with multiple appointments with an orthotist/prosthetist needed for each prosthetic. The process hurts patients that are children the most, since during the lengthy time taken to the manufacture of a prosthetic (can take several months) the child could grow significantly enough for the initial measurements to be wrong [21]. As a reference, a rough total cost of the setup for automated scanning described in this work is listed below:

- ABB IRB 1200 robot arm – €25,000.
- HandyScan 700 (2015 ed.) – €28,500.
- Mid-range FFF printer, supporting thermoplastic polyurethane (TPU) – €5,000.
- Software licenses – €5,000 or more.
- Design and manufacturing of multiple-sized sleeves with markers pre-applied – <€1,000.
- Total initial capital needed is more or less €65,000.

The traditional method for capturing a patient's stump measurements is plaster casting, which involves wrapping it in plaster-impregnated bandages that have to soak in water, placed carefully layer by layer and then drying [27]. Whole process can take anywhere from 15 to 30 minutes, with an additional time of several hours before the mould can be used in further manufacturing, which is significantly longer than the 2 minutes average achieved in the automated 3D scanning setup. As discussed in various online sources, traditional plaster casting can take several orthotist appointments to get the right fit, causing not only more material waste but also increased travel costs. Average cost of measurement is provided in a table below (Table 9**.** Estimated Cost of Stump Measurement), where estimated wage of an orthotist was taken as €45/h and €30/h for the technician, manufacturing costs were not included as they depend on the prosthetic type and individual order. Technician work time of 1 hour was included as that is how long it takes to dry the mould, for the automatic method, technician labour involves preparing and maintaining the printing bed.

Table 9. Estimated Cost of Stump Measurement

Cost Source	**Traditional plaster casting**	**Automated scan with FFF printing**
Orthotist labour	$0.25\ h \cdot €45/\text{h} = €12.25$	$0.035\ h \cdot €45/\text{h} = €1.575$
Technician labour	$1\ h \cdot €30/\text{h} = €30$	$0.2\ h \cdot €30/\text{h} = €6$
Disposable material	Plaster, stockinette, foam = €25	Markers (reusable), IPA wipes = €2
Patient travel (only counted beyond 1)	€30	€0
Total	€97.25	€9.575

The very rough estimation already highlights a difference of 10 times in cost per cast, as the automated method is much faster and does not use any material for measuring, making it more sustainable also. Though not currently possible, cost and emissions could be reduced much more by eventually introducing completely automated scanning that could be done at most clinics, which would cut out the need to have orthotist appointments, removing travel time from the list. This type of innovation would require cheaper cost of setup though, which is not currently feasible. A number of 31,000 prosthetics is estimated to be sold each year, so as an example for calculation, a clinic that produces or orders the production of at least 400 prosthetic devices per year will be assumed as the target for implementing automated scanning. According to calculations, €35,070 would be saved at such sales per year, this would lead to break even within 3 years, which is also visualised in a cumulative savings figure (Fig. 40). While 3 years is not a bad time to make the investment back, it can be even faster if more sales are done per year, for example, to break even within one year 742 prosthetics would have to be made. This was still a conservative estimate as other more detailed costs are not included, such as mould storage space, transportation, employee count among others. If completely remote scanning is considered (not feasible currently), cost could go down to as low as ~€1-5 per unit due to the removed travel cost, but travel cost was not assessed in detail here, so it is not considered.

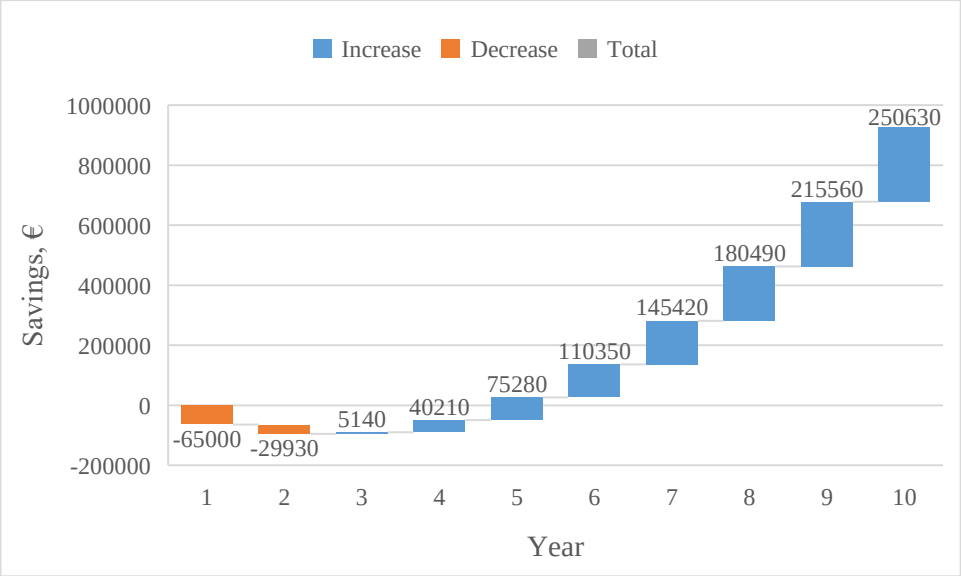

Fig. 40. Cumulative Savings (€) Per Year if Yearly Sales Are 400

Besides monetary gain, the environmental effects of switching to 3D scanning as the method of measurement are profound. In the process of plaster casting, several kilograms of waste are generated per patient [28, 33] the moulds are not reusable or even directly recyclable, resulting in tons of wasted toxic material every year, polluting the environment. If all 31,000 prosthetics per year were made using 3D scanning for measurement this would suggest that at least 62 tons of plaster waste could be saved every year globally, assuming that all of them are made by plaster casting (not likely). The alternative 3D scanning method has no waste whatsoever other than electricity consumption, even if 3D printing via FFF is also included in the waste, skin-safe materials like TPU are recyclable. These factors, along with the price reduction make automated scanning a better choice than traditional methods. An interesting fact is that prices of the type of scanner used in the study have not gone down in the last 10 years, in fact, they have not changed, but the scanners have improved in both weight

and parameters, accounting for inflation also shows that they have reduced in relative value by about 20 %.

4.2. Chapter Summary

Total cost of one-time setup was estimated to be around €65,000, which is out of reach for the average individual, but entirely viable for a clinic of moderate size that specializes in some part in the prosthetic production field. A rough calculation using estimates showed that switching from the traditional method of plaster casting moulds to automated 3D scanning workflow could save ~€85 per unit, resulting in first year profit if 742 units are made within a year (only feasible for a very large clinic). Several kilograms of average plaster waste are generated per prosthetic made, which is not a recyclable material resulting in pollution. For the mentioned 742 units – at least 1,5 tons of plaster waste would be avoided by switching to 3D scanning as the method of measurement.

Conclusions

1. A two-part adapter was modelled by first scanning the HandyScan 700 using a different scanner, cleaning the scan and using it as reference, adapter was fabricated using PLA material, secured by M5 bolts, no issues arose in mounting or scanning.
2. Custom rapid code was prepared for driving robot motion at a constant 335 mm distance to the object, never exceeding the manufacturer's velocity or joint torque limits, the emergency safety mechanisms were never triggered during the tests.
3. The system was made extremely adaptable due to the various scanner settings and custom code, where all distances can be modified along with speeds, resolution, number of passes and others, the best settings found can be extrapolated to other laser scanners, or even to structured light scanners.
4. After comparing, best results were retrieved at 0.2 mm resolution, 100 mm/s speed, where SD was measured at 0.039 mm on average, with scanner noise of 0.0277 mm; speed to quality wise, 0.6 mm resolution at 800 mm/s speed achieved 0.057 mm SD as the best compromise, this was a better result than most other analysed works.
5. Initial investment to deploy the system is approx. €65,000, cutting labour and waste costs by €87 per stump measured via 3D scanning system rather than plaster casting; assuming 2 kg plaster waste per patient, a large clinic selling 742 prosthetics per year could prevent around 1,500 kg of polluting waste yearly, a substantial environmental effect.

List of References

1. IDREES, Sadia; GILL, Simeonand VIGNALI, Gianpaolo. Mobile 3D Body Scanning Applications: A Review of Contact-Free AI Body Measuring Solutions for Apparel. The Journal of the Textile Institute, 2024, vol. 115, no. 7. pp. 1161–1172. Available from <https://doi.org/10.1080/00405000.2023.2216099>. ISSN 0040-5000.
2. JAVAID, Mohd, et al. Industrial Perspectives of 3D Scanning: Features, Roles and It's Analytical Applications. Sensors International, 2021, vol. 2. pp. 100114. Available from <https://www.sciencedirect.com/science/article/pii/S2666351121000358>. ISSN 2666-3511.
3. ESAIAS, Owen, et al. Improved Area of Origin Estimation for Bloodstain Pattern Analysis using 3D Scanning. Journal of Forensic Sciences, 20191203, May, 2020, vol. 65, no. 3. pp. 722–728. ISSN 1556-4029; 0022-1198.
4. MATYS, Marian; KRAJCOVIC, Martinand GABAJOVA, Gabriela. Application of 3D Scanning for the Creation of 3D Models Suitable for Immersive Virtual Reality. Zarządzanie Przedsiębiorstwem. Enterprise Management, 2023. Available from <https://search.datacite.org/works/10.25961/ent.manag.26.02.02>.
5. KIHARA, Hidemichi, et al. Accuracy and Practicality of Intraoral Scanner in Dentistry: A Literature Review. Journal of Prosthodontic Research, Apr 1, 2020, vol. 64, no. 2. pp. 109–113. Available from <https://dx.doi.org/10.1016/j.jpor.2019.07.010> J-STAGE of NDL. ISSN 1883-1958.
6. KIM, Bo Ryun, et al. Efficacy of a Hip Brace for Hip Displacement in Children with Cerebral Palsy: A Randomized Clinical Trial. JAMA Network Open, 2022, vol. 5, no. 11. pp. e2240383. Available from <https://doi.org/10.1001/jamanetworkopen.2022.40383>. ISSN 2574-3805.
7. KAUSHIK, Ashish, et al. Advanced 3D Body Scanning Techniques and its Clinical Applications. Piscataway: IEEE, Dec 2022. Available from <https://ieeexplore.ieee.org/document/10097041>.
8. RUDARI, Michele, et al. Accuracy of Three-Dimensional Scan Technology and its Possible Function in the Field of Hand Surgery. Plastic and Reconstructive Surgery - Global Open, 2024, vol. 12. pp. e5745.
9. BARTOL, K., et al. A Review of Body Measurement using 3D Scanning. IEEE Access, 2021, vol. 9. pp. 67281–67301. ISSN 2169-3536.
10. YANG, Yusheng, et al. The Development of a Low-Cost Photogrammetry-Based 3D Hand Scanner. HardwareX, 2021, vol. 10. pp. e00212. Available from <https://www.sciencedirect.com/science/article/pii/S2468067221000419>. ISSN 2468-0672.
11. NUZZI, Cristina, et al. Body Measurement Estimations using 3D Scanner for Individuals with Severe Motor Impairments. Piscataway: IEEE, Jun 14, 2023. Available from <https://ieeexplore.ieee.org/document/10171946>.
12. CIMOLIN, Veronica, et al. The Smart Body Concept as a Demonstration of the Overarching Utility and Benefits of 3D Avatars in Retail, Health and Wellbeing: An Accuracy Study of Body Measures from 3D Reconstruction. Multimedia Tools and Applications, Mar 1, 2023, vol. 82, no. 7. pp. 11079–11098. Available from <https://link.springer.com/article/10.1007/s11042-022-13661-x> PubMed. ISSN 1380-7501.

13. ZERAATKAR, Mojtaba; and KHALILI, Khalil. A Fast and Low-Cost Human Body 3D Scanner using 100 Cameras. Journal of Imaging, Apr 9, 2020, vol. 6, no. 4. pp. 21. Available from <https://www.proquest.com/docview/2389371665> CrossRef. ISSN 2313-433X.
14. TROJNACKI, Maciej; DĄBEK, Przemysławand JAROSZEK, Piotr. Mechatronic Design and Experimental Research of an Automated Photogrammetry-Based Human Body Scanner. Sensors (Basel, Switzerland), Jun 23, 2023, vol. 23, no. 13. pp. 5840. Available from <https://www.ncbi.nlm.nih.gov/pubmed/37447690> MEDLINE. ISSN 1424-8220.
15. PELLITTERI, Federica, et al. Accuracy of 3D Facial Scans: A Comparison of Three Different Scanning System in an in Vivo Study. Progress in Orthodontics, 2023, vol. 24.
16. MAJOR, Martin, et al. Evaluation of a Structured Light Scanner for 3D Facial Imaging: A Comparative Study with Direct Anthropometry. Sensors, 2024, vol. 24, no. 16. ISSN 1424-8220.
17. YU, Fang, et al. Evaluating the Accuracy of Hand Models obtained from Two 3D Scanning Techniques. Scientific Reports, 2020, vol. 10, no. 1. pp. 11875. Available from <https://doi.org/10.1038/s41598-020-68457-6>. ISSN 2045-2322.
18. SCHIPPER, J. A. M., et al. Reliability and Validity of Handheld Structured Light Scanners and a Static Stereophotogrammetry System in Facial Three-Dimensional Surface Imaging. Scientific Reports, 2024, vol. 14, no. 1. pp. 8172. Available from <https://doi.org/10.1038/s41598-024-57370-x>. ISSN 2045-2322.
19. POWERS, Olivia A.; PALMER, Jeff R.and WILKEN, Jason M. Reliability and Validity of 3D Limb Scanning for Ankle-Foot Orthosis Fitting. Prosthetics and Orthotics International, Feb 1, 2022, vol. 46, no. 1. pp. 84–90. ISSN 1746-1553; 0309-3646; 0309-3646.
20. FARHAN, Muhannad, et al. Comparison of Accuracy and Speed between Plaster Casting, High-cost and Low-cost 3D Scanners to Capture Foot, Ankle and Lower Leg Morphology of Children Requiring Ankle-foot Orthoses. Journal of Foot and Ankle Research, 2024, vol. 17.
21. GÓRSKI, Filip, et al. Study on Properties of Automatically Designed 3D-Printed Customized Prosthetic Sockets. Materials (Basel, Switzerland), 20210912, Sep 12, 2021, vol. 14, no. 18. pp. 5240. doi: 10.3390/ma14185240. ISSN 1996-1944; 1996-1944; 1996-1944.
22. CUTTI, Andrea Giovanni, et al. Accuracy, Repeatability, and Reproducibility of a Hand-Held Structured-Light 3D Scanner Across Multi-Site Settings in Lower Limb Prosthetics. Sensors (Basel, Switzerland), 20240407, Apr 7, 2024, vol. 24, no. 7. pp. 2350. doi: 10.3390/s24072350. ISSN 1424-8220; 1424-8220.
23. Kreon 3D. (2025, April 4th). How does laser triangulation 3d scanning technology improve manufacturing processes? https://www.kreon3d.com/article/how-does-laser-triangulation-3d-scanning-technology-improve-manufacturing-processes
24. VOGT, Maximilian; RIPS, Adrianand EMMELMANN, Claus. Comparison of iPad Pro®'s LiDAR and TrueDepth Capabilities with an Industrial 3D Scanning Solution. Technologies (Basel), Apr 7, 2021, vol. 9, no. 2. pp. 25. Available from <https://search.proquest.com/docview/2544546001> CrossRef. ISSN 2227-7080.
25. ABB Group. (2025, April 4th). Product specification – IRB 120. https://library.e.abb.com/public/b3f54da20003467c8a06ab452d50a09c/3HAC081417%20PS%20IRB%201200%20on%20OmniCore-en.pdf
26. ABB Group. (2025, April 4th). Technical reference manual – RAPID Instructions, Functions and Data types. https://library.e.abb.com/public/b227fcd260204c4dbeb8a58f8002fe64/Rapid_instructions.pdf

27. CHOO, Yoo Jin; KIM, Du Hwanand CHANG, Min Cheol. Amputation Stump Management: A Narrative Review. World Journal of Clinical Cases, May 6, 2022, vol. 10, no. 13. pp. 3981–3988. Available from <https://www.ncbi.nlm.nih.gov/pubmed/35665133> CrossRef. ISSN 2307-8960.
28. SHIYO, Servas; NAGELS, Jozefand SHANGALI, Harold G. Recycling of Plaster of Paris. African Journal of Disability, Jan 1, 2020, vol. 9, no. 3. ISSN 2223-9170.
29. MA, Qianli, et al. Learning to Dress 3D People in Generative Clothing. 2020 IEEE/CVF Conference on Computer Vision and Pattern Recognition (CVPR), Jun, 2020. pp. 6468-6477. Available from <https://ieeexplore.ieee.org/document/9157608>.
30. ZHAO, Ran, et al. PoseNormNet: Identity-Preserved Posture Normalization of 3-D Body Scans in Arbitrary Postures. IEEE Transactions on Industrial Informatics, Nov 1, 2023, vol. 19, no. 11. pp. 11298-11309. Available from <https://search.proquest.com/docview/2866492249> CrossRef. ISSN 1551-3203.
31. BATOOL, Raheela; and MOU, Jian. A Systematic Literature Review and Analysis of Try-on Technology: Virtual Fitting Rooms. Data and Information Management, 2024, vol. 8, no. 2. pp. 100060. Available from <https://www.sciencedirect.com/science/article/pii/S2543925123000347>. ISSN 2543-9251.
32. SHESHTAR, Fatemah M., et al. Comparative Analysis of LiDAR and Photogrammetry for 3D Crime Scene Reconstruction. Applied Sciences, 2025, vol. 15, no. 3. ISSN 2076-3417.
33. POLLICE, Bella; THIEL, Cassandra L.and BARATZ, Mark E. Life Cycle Assessment in Orthopedics. Operative Techniques in Orthopaedics, Dec, 2022, vol. 32, no. 4. pp. 100998. Available from <https://dx.doi.org/10.1016/j.oto.2022.100998> CrossRef. ISSN 1048-6666.

Appendices

Appendix 1. RAPID code for robot movement

```
MODULE MainModule
   !This code is for changing radius before every arc drawn, each arc has a peak that is half of r1. The scanner is made to follow a point below the center of the circle radius.
   !Variables
   VAR num z0 := 350;       ! Height position of surface
   VAR num b := 0.1;        ! Radius decrement per lap
   VAR num r1 := 435;       ! Current radius
   VAR num Rmax := 435;     ! Max radius
   VAR num Rmin := 435;     ! Min radius
   VAR num y0 := 0;         ! Circle center Y
   VAR num x0 := 250;       ! Circle center X
   VAR num started := 0;    ! Tracks if the robot was positioned already
   VAR speeddata speed := v100; ! Sets robot movement speed to a preset
   VAR speeddata transition := v100; ! sets speed of transition movements

   !Coordinate points assigned later
   VAR num z1; VAR num y1;
   VAR num z2; VAR num y2;
   VAR num z3; VAR num y3;
   VAR num z4; VAR num y4;
   VAR num z5; VAR num y5;

   !Angle phi and quaternions
   VAR num phi;
   VAR num phi2;

   !robot 'targets', e.g. points to move towards
   VAR robtarget target1;
   VAR robtarget target2;
   VAR robtarget target3;
   VAR robtarget target4;

   !tool dir
   VAR orient qDown;
   VAR orient q1;
   VAR orient q2;

   PROC main()
      ! Generate 5 circular points based on radius
      y1 := r1 * sin(-90) + y0; z1 := r1 * cos(-90) + z0;
      y2 := 5*r1/6 * sin(0) + y0; z2 := 5*r1/6 * cos(0) + z0;
      y3 := r1 * sin(90) + y0; z3 := r1 * cos(90) + z0;
```

```
y4 := 5*r1/6 * sin(0) + y0; z4 := 5*r1/6 * cos(0) + z0;
y5 := r1 * sin(-90) + y0; z5 := r1 * cos(-90) + z0;
qDown := OrientZYX(0,180,0);
AccSet 20, 20;
IF started = 0 THEN
   ! Move to start position
   phi := -Atan2((y0 - y1), (-300 - z1));
   phi2 := -Atan2((x0 - 25), (y0 + y1));
   q1 := OrientZYX(phi2/6,180,phi/2);
   ConfL \Off;
   MoveL [[x0, y0, z2],  qDown, [-1,-1,-1,0],
   [9E9,9E9,9E9,9E9,9E9,9E9]], transition, z20, tool0;
   MoveL [[x0, y1, z2/2],  q1, [-1,-1,-1,0],
   [9E9,9E9,9E9,9E9,9E9,9E9]], transition, z20, tool0;
   MoveL [[x0, y1, z1],  q1, [-1,-1,-1,0],
   [9E9,9E9,9E9,9E9,9E9,9E9]], v50, z20, tool0;
   started := 1;

ELSEIF r1 >= Rmin THEN
   !Dez20 parameters of each target
   phi := -Atan2((y0 - y2), (-300 - z2));
   phi2 := Atan2((x0 - 25), (y0 - y2));
   q1 := OrientZYX(phi2/6, 180, 0);
   target1.trans := [x0, y2, z2];
   target1.rot   := q1;
   target1.robconf := [-1,-1,-1,0];
   target1.extax   := [9E9,9E9,9E9,9E9,9E9,9E9];

   phi := -Atan2((y0 - y3), (-300 - z3));
   phi2 := Atan2((x0 - 25), (y0 - y3));
   q2 := OrientZYX(phi2/6, 180, phi/2);
   target2.trans := [x0, y3, z3];
   target2.rot   := q2;
   target2.robconf := [-1,-1,-1,0];
   target2.extax   := [9E9,9E9,9E9,9E9,9E9,9E9];

   ! Draw arc
   ConfL \Off;
   MoveC target1, target2, speed, fine, tool0;
   q2 := OrientZYX(phi2/8, 180, phi/2);
   MoveL [[x0+120, y3, z3],  q2, [-1,-1,-1,0],
   [9E9,9E9,9E9,9E9,9E9,9E9]], transition, z20, tool0;

   !Second arc params
   phi := -Atan2((y0 - y4), (-300 - z4));
   phi2 := -Atan2((x0 - 25), (y0 - y4));
```

```
q1 := OrientZYX(phi2/8, 180, 0);
target3.trans := [x0+120, y4, z4];
target3.rot   := q1;
target3.robconf := [-1,-1,-1,0];
target3.extax   := [9E9,9E9,9E9,9E9,9E9,9E9];

phi := -Atan2((y0 - y5), (-300 - z5));
phi2 := -Atan2((x0 - 25), (y0 + y5));
q2 := OrientZYX(phi2/8, 180, phi/2);
target4.trans := [x0+120, y5, z5];
target4.rot   := q2;
target4.robconf := [-1,-1,-1,0];
target4.extax   := [9E9,9E9,9E9,9E9,9E9,9E9];

!Draw 2nd arc
ConfL \Off;
MoveC target3, target4, speed, fine, tool0;
q2 := OrientZYX(phi2/7, 180, phi/2);
MoveL [[x0+240, y5, z5],  q2, [-1,-1,-1,0],
[9E9,9E9,9E9,9E9,9E9,9E9]], transition, z20, tool0;

!Third arc params
phi := -Atan2((y0 - y2), (-300 - z2));
phi2 := Atan2((x0 - 25), (y0 - y2));
q1 := OrientZYX(phi2/7, 180, 0);
target1.trans := [x0+240, y2, z2];
target1.rot   := q1;
target1.robconf := [-1,-1,-1,0];
target1.extax   := [9E9,9E9,9E9,9E9,9E9,9E9];

phi := -Atan2((y0 - y3), (-300 - z3));
phi2 := Atan2((x0 - 25), (y0 - y3));
q2 := OrientZYX(phi2/7, 180, phi/2);
target2.trans := [x0+240, y3, z3];
target2.rot   := q2;
target2.robconf := [-1,-1,-1,0];
target2.extax   := [9E9,9E9,9E9,9E9,9E9,9E9];

! Draw 3rd arc
ConfL \Off;
MoveC target1, target2, speed, fine, tool0;

!Reduce radius
r1 := r1 - b/2;
y1 := r1 * sin(-90) + y0; z1 := r1 * cos(-90) + z0;
y2 := r1 * sin(0) + y0; z2 := r1 * cos(0) + z0;
```

```
            y3 := r1 * sin(90) + y0; z3 := r1 * cos(90) + z0;
            y4 := r1 * sin(0) + y0; z4 := r1 * cos(0) + z0;
            y5 := r1 * sin(-90) + y0; z5 := r1 * cos(-90) + z0;

            !Adjustment of position after radius change
            ConfL \Off;
            q2 := OrientZYX(phi2/6, 180, phi/2);
            MoveL [[x0, y3, z3],  q2, [-1,-1,-1,0], [9E9,9E9,9E9,9E9,9E9,9E9]], transition, z20, tool0;

        ELSE
            !Move away after finished
           MoveL [[x0, 0, 750], qDown, [-1,-1,-1,0], [9E9,9E9,9E9,9E9,9E9,9E9]], transition, z20, tool0;
            Stop;
        ENDIF

    ENDPROC

ENDMODULE
```